

# **Stability analysis of low- $n$ modes for the Divertor Tokamak Test facility Single Null Scenario**

Valeria Fusco, Gregorio Vlad, Giuliana Fogaccia, Edmondo Giovannozzi

- The work has been developed during 2021 for the DTT MHD Task and it has been presented during the final meeting related to the task
- Abstract for the incoming 48th EPS Conference as poster contribution



Stability analysis of low-n modes for the Divertor Tokamak Test facility

Single Null Scenario

V. Fusco<sup>1</sup>, G. Vlad<sup>1</sup>, G. Fogaccia<sup>1</sup>, E. Giovannozzi<sup>1</sup>

ENEA, FSN, C. R. Frascati, Via E. Fermi 45, 00044 Frascati (Roma), Italy

Stability analysis is considered to be of fundamental importance to allow operation of plasma fusion devices and prevent bad confinement with consequent loss of plasma performance and/or plasma wall damages. For these reasons a careful analysis of the plasma stability properties for the DTT (Divertor Tokamak Test) machine [1] is undergoing. DTT is a new facility, under construction in Frascati, Italy, whose aim is to design and test a divertor able to face the problems of thermal loads and power exhaust. In this work the SN (single null) scenario proposed for DTT is studied [2]; our attention is focused on low-n stability for both ideal and resistive plasmas. Such analysis is part of a process where different codes follow each other in a consistent chain; so, equilibrium analysis, which precedes stability, follows the results of electromagnetic analyses (CREATE-NL, [3]) and transport analyses (JETTO, [4]). The code used to study the equilibrium is CHEASE [5], a high-resolution fixed boundary code that solves the Grad-Shafranov equation in toroidal geometry, assuming static MHD equilibria and axisymmetry. MARS [6] is the stability code used. It solves full MHD linear, resistive equations and can also consider a vacuum zone between the plasma last closed surface and a perfectly conducting wall, which is conformal to the plasma last closed magnetic surface. First the reference scenario is carefully analyzed; in this framework, the relevant parameters are the safety factor on axis,  $q_0=0.7$ , and at the edge,  $q_{95\%}=2.8$ , the  $q=1$ , located around  $s \approx 0.64$  (being  $s$  the poloidal radial like coordinate), the  $\beta=1.9$ , defined as  $2\mu_0\langle p \rangle / B_0$ , being  $p$  the pressure averaged on the plasma volume and  $B_0$  the on axis magnetic field, the pressure peaking approximately equal to 4. Studies with ideally conducting wall placed at infinity as well as at finite distance have been considered. Moreover  $\beta$  and safety factor profiles have been varied to perform a sensitivity study. The analysis reveals, for the reference scenario, an unstable internal kink ( $m,n)=(1,1)$ , and infernal modes localized around the low shear and high pressure gradient zone. No external modes were observed unless main quantities, such as the safety factor or the  $\beta$  parameter, are strongly varied.

[1] R. Martone, R. Albanese, F. Crisanti, A. Pizzuto, P. Martin. "DTT Divertor Tokamak Test facility Interim Design Report, ENEA (ISBN 978-88-8286-378-4), April 2019 ("Green Book")" <https://www.dtt-dms.enea.it/share/s/avvglhVQT2aSkSgV9vuEtw>. [2] Casiraghi et al, Nucl.Fusion 61, 2021, 116068. [3] R. Albanese et al., Fusion Engineering and Design 96–97 (2015) 664–667. [4] Cenacchi G. and Taroni A. 1988 ENEA-RT-TIB 88-5 ENEA. [5] H. Lütjens, et al., 97, Issue 3, 1996, Pages 219-260. [6] A. Bondeson, G. Vlad, and H. Lütjens. Physics of Fluids, B4:1889–1900, 1992.

# Outline

## Introduction

- Aim of the study

Summary of results obtained (i) and how they have been approached(ii):

- Ideal stability
- Resistive stability
- Sensitivity analysis

} from low to intermediate toroidal mode number  $n$

## Aim of the study

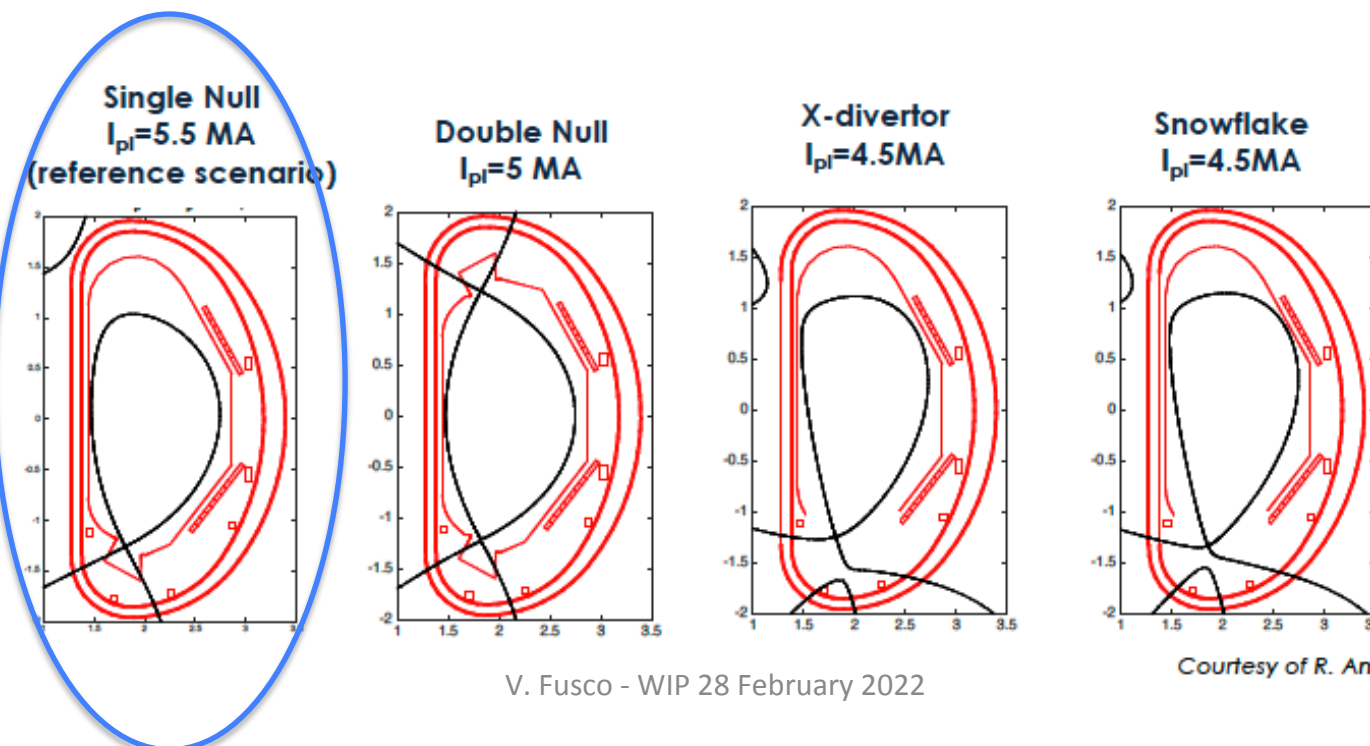
- ✓ Investigate, from a stability point of view, DTT scenarios

Different reference equilibria have been analyzed which have similar characteristic as concern stability. In particular, the following analysis focuses on the reference scenario:  
final\_eqdskfile\_PPFseq2196\_DTT2021\_02567.

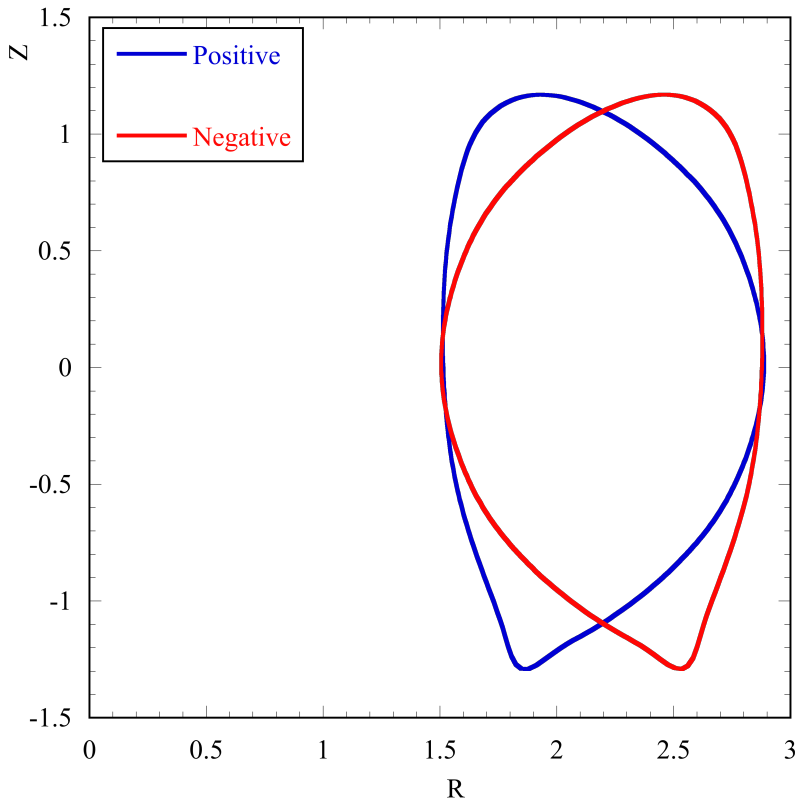
Stability analysis is considered to be of fundamental importance to allow operation of plasma fusion devices and prevent bad confinement with consequent loss of plasma performance and/or plasma wall damages.

The scenario analyzed has the following characteristics:

- Single Null (SN)



- Positive Triangularity (PT)



### DTT main parameters

$a$  = 0.70 m  
 $R_0$  = 2.19 m  
 $B_0$  = 5.85 T  
 $I_p$  = 5.5 MA  
 $P_{tot}$  = 45 MW  
 $n_e$   $\approx$  2.4  $10^{20}$  m $^{-3}$   
 $T_e$   $\approx$  15 keV  
 $T_i$  = 9.5 keV

- Full Power Scenario



7 MW

**Day 0**

3T/2.0MA



25 MW

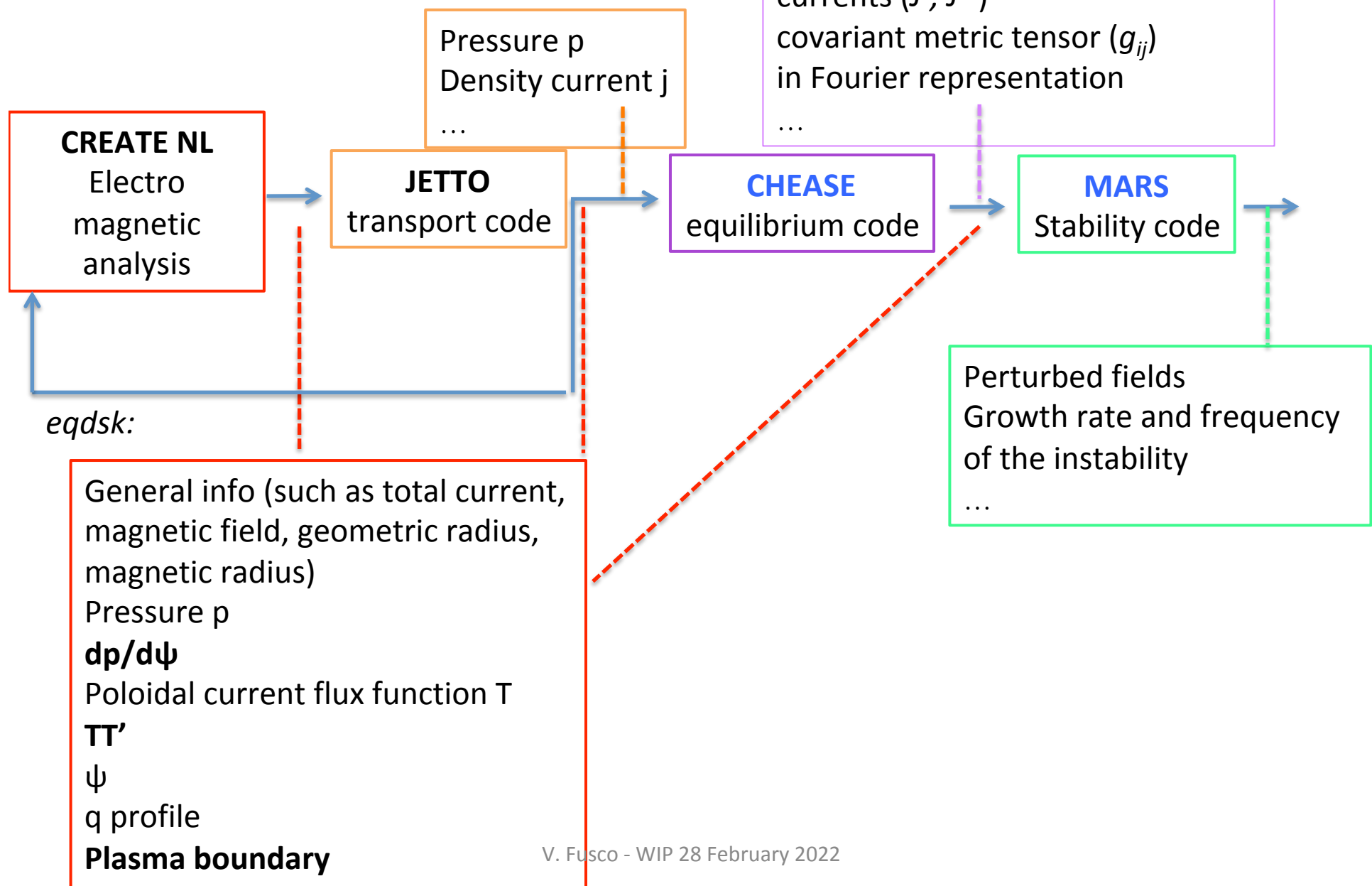
**Day 1**

5.85T/4.0MA



- MHD Stability analysis in this study focus on:
- ✓ Mainly **Ideal** stability, indeed ideal MHD stability evolves on the rapid Alfvén time scale so that they can be catastrophic for plasma confinement
- ✓ **Resistive stability.** Resistivity removes constraints from the ideal equation adding new modes to stability scenario. Anyway, resistive instabilities generally grow on a time scale much slower than the Alfvén time. [R. White [1] , G. Bateman [2]]

# Codes used for the analysis: **MARS and CHEASE**



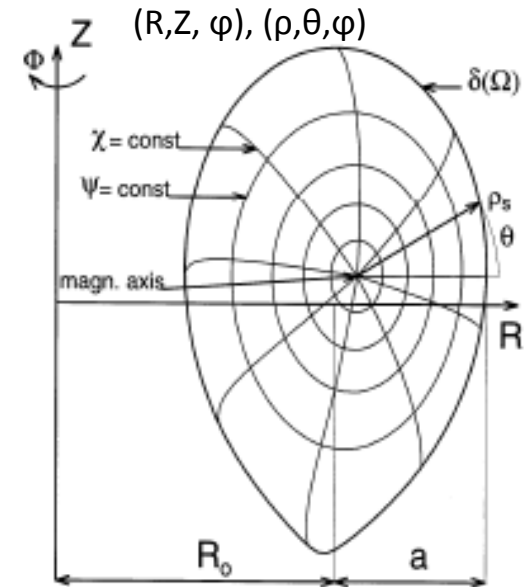
# Equilibrium -> CHEASE

H. Lütjens, A. Bondeson, O. Sauter [3]

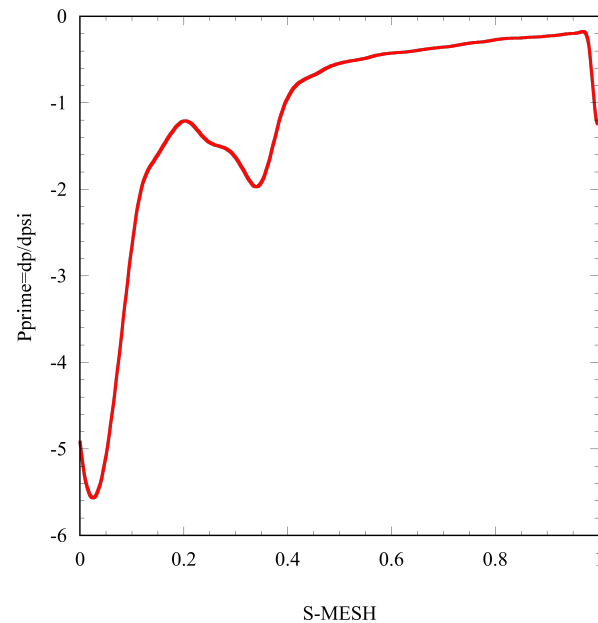
The code solves the Grad-Shafranov equation in toroidal geometry

$$\nabla \cdot \frac{1}{R^2} \nabla \psi = \frac{j_\Phi}{R} = -p'(\psi) - \frac{1}{R^2} T T'(\psi)$$

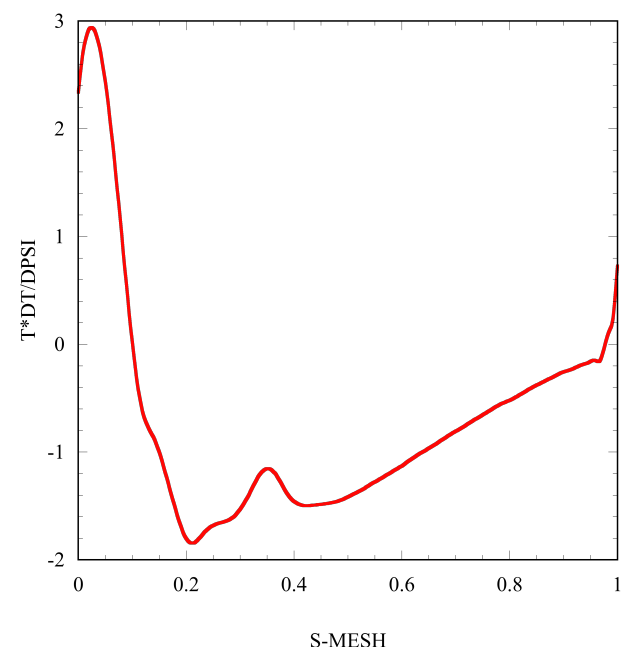
$$\underline{B} = T \nabla \phi + \nabla \phi \times \nabla \psi$$



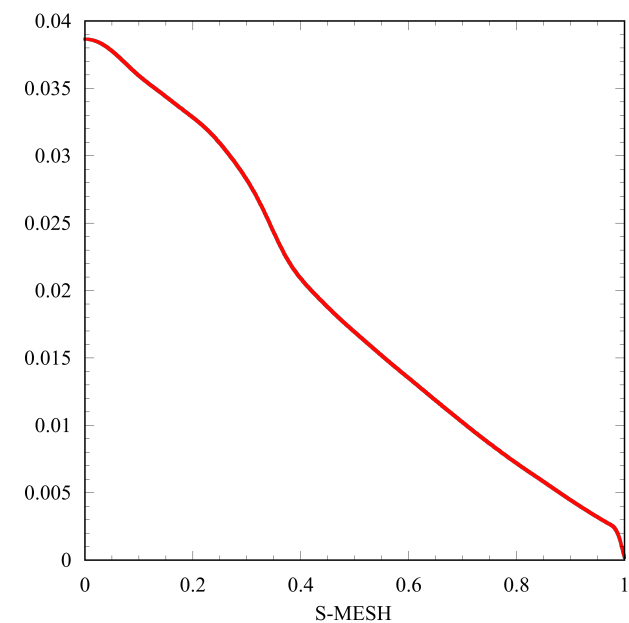
$$p'(s) = dp/d\psi$$



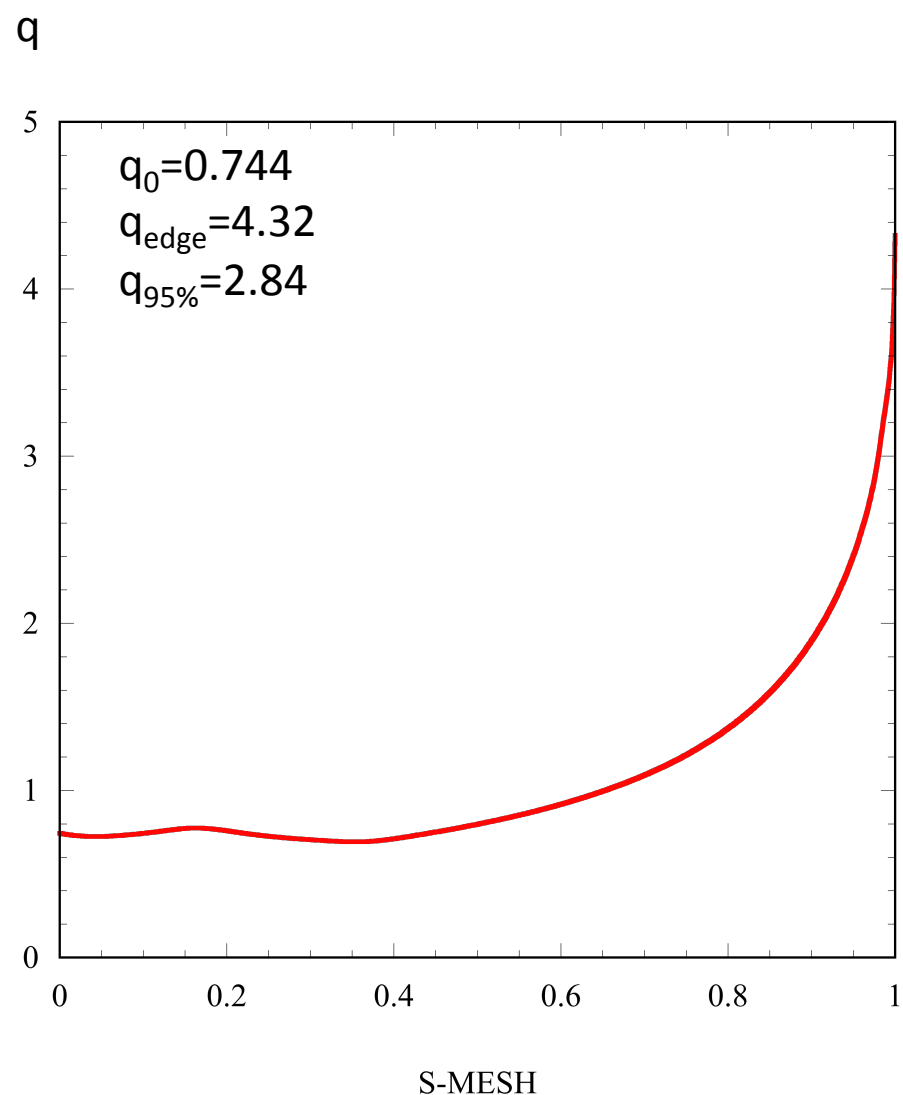
$$T T'(s) = T dT/d\psi$$



Pressure -> 1.05 Pa on axis  
pressure peaking =  $p_0/\langle p \rangle \approx 4$

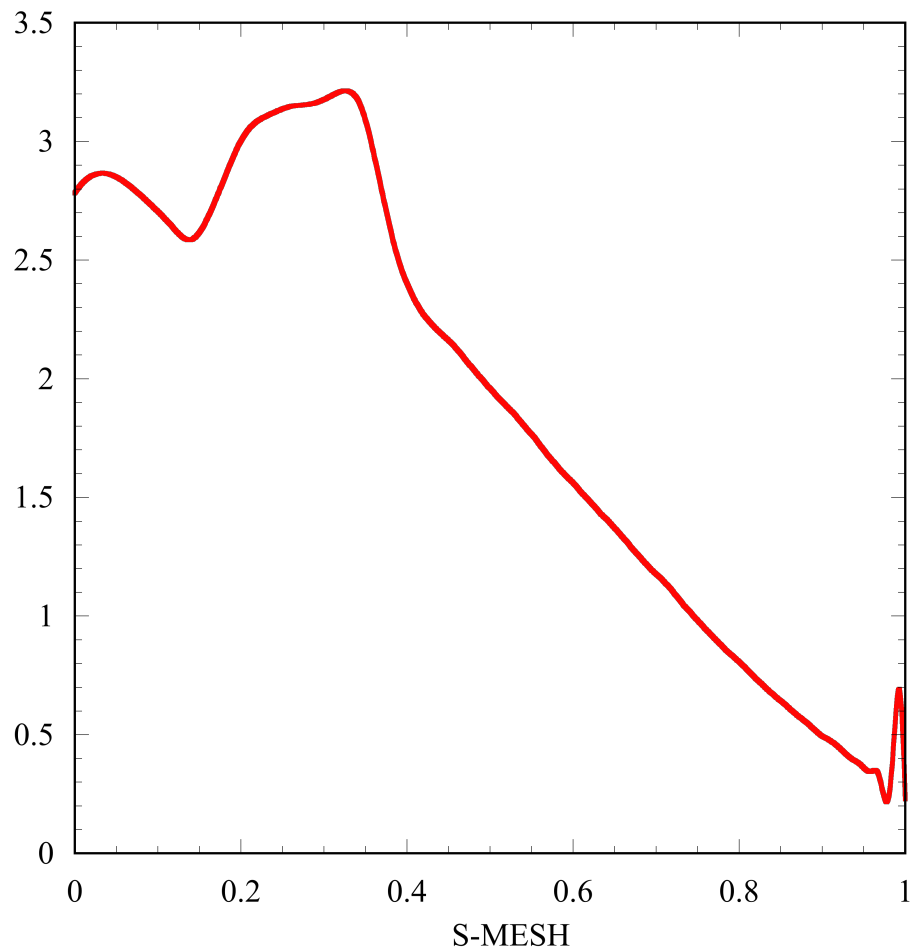


Safety factor profile



Surface averaged current density obtained by  
CHEASE

$$I^* = \langle j_{\text{phi}} / R \rangle / \langle 1 / R \rangle \mu_0 R_0 / B_0$$



## Stability analysis ->MARS

A. Bondeson, G. Vlad, and H. Lütjens [4]

It solves **full MHD linear, resistive** equations [ A. Bondeson, G. Vlad, and H. Lütjens [4]].

It considers a two dimensional, **axisymmetric** general **toroidal** geometry carried out in **flux coordinate**  $(s, \chi, \phi)$  where  $s = (1 - \psi / \psi_{\text{axis}})^{1/2}$  is the radial-like coordinate,  $\psi$  is the poloidal flux function,  $\chi$  is a generalized poloidal angle and  $\phi$  is the geometrical toroidal angle.

It is a **spectral code**, that is, it solves the MHD equation in the Fourier space of the toroidal and poloidal coordinates.

The  $s$  radial like coordinates is, instead, solved with the finite elements technique

It can consider a **vacuum** zone between the plasma last closed surface and a perfectly conducting wall which is conformal to the plasma. This conducting wall can be placed on the plasma surface as well.

Output relevant quantities

Perturbed fields  
Growth rate and frequency  
of the instability

## Summary of results obtained

**Ideal modes** revealed in the analysis:

- **Internal kink**  $(m,n)=(1,1)$ ,  $q=1$  rational surface localized around a large radius  $\approx 0.6$
- **Infernal modes** [Manickam [5]] from low to intermediate toroidal  $n$  and poloidal  $m$  mode numbers, localized around the **low shear** and **high gradient pressure** zone. They are **pressure driven** internal MHD instabilities that are excited in a region of **low shear**.

Note that when profiles do not admit infernal modes, ballooning modes are considered the most limiting modes, unless  $q_0 < 1$  in which case the  $n=1$  internal kink may be more restrictive.

If infernal modes are present then a moderate  $n$  may be the most unstable, anyway this value of  $n$  is profile dependent and the growth rate has an oscillatory behaviour with respect to  $n$  and thus it is difficult to predict which mode number will be the most unstable.

**Resistive modes** revealed in the analysis:

- **Resistive internal kink**  $(m,n)=(1,1)$ .
- No evidence of tearing modes  $(m,n)=(2,1)$  or  $(m,n)=(3,2)$ .

No **external mode** observed for this equilibrium

**Sensitivity** analysis on relevant quantities such as the  $q_0$  and  $\beta$  show [Turnbull [7], Buttery [8], Fasoli [9]]:

- Internal kink is switched on as long as the  $q_0 < 1$ .
- Infernal modes are still revealed as long as the  $q$  rational surfaces are in a low shear and high pressure gradient zone
- For  $q_0 > 1$  or high  $\beta$ , external modes have been found

**Convergences** test have been executed to confirm the analysis.

## Stability analysis with MARS for the reference scenario: ideal study

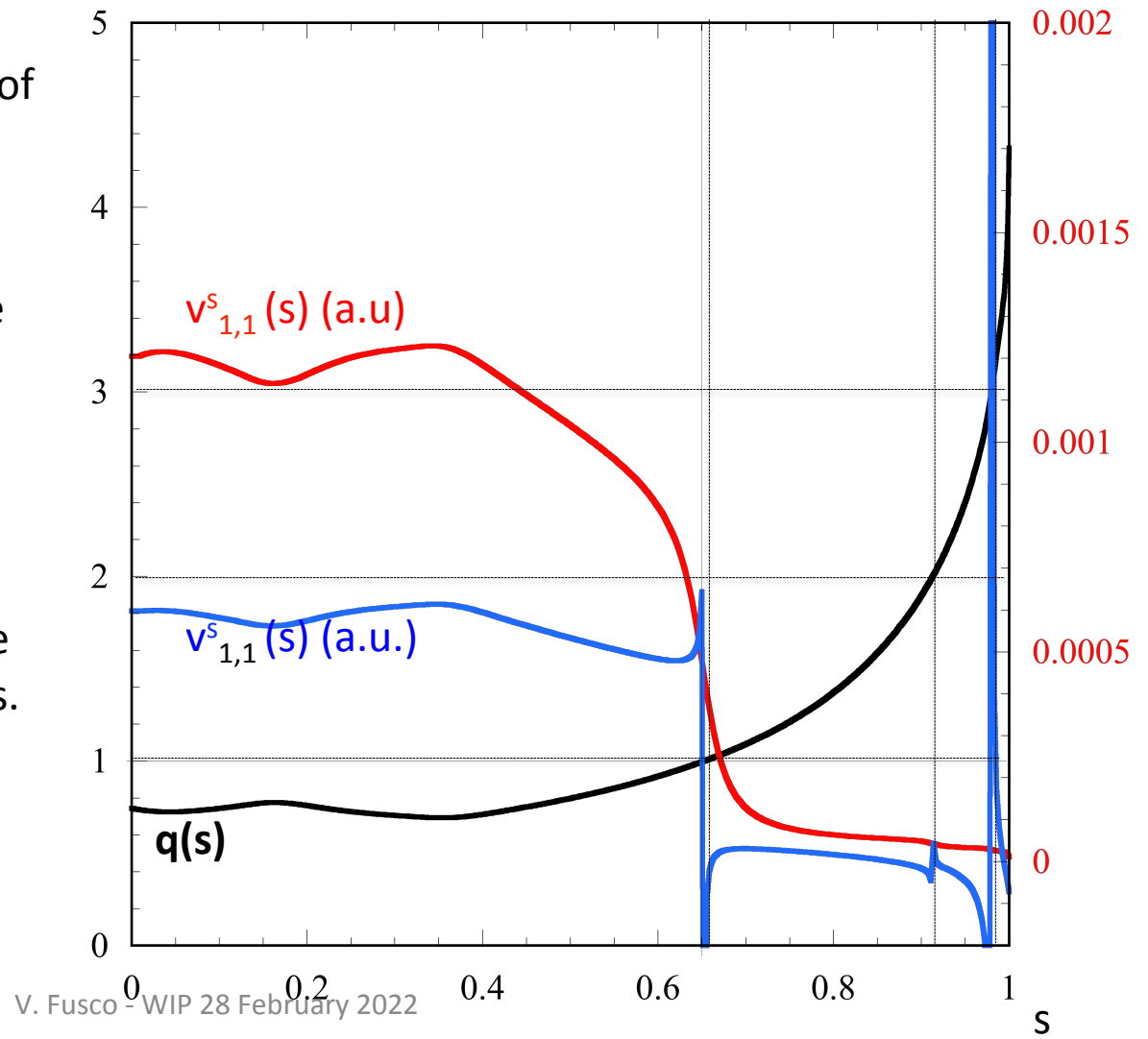
- ✓ A  $(m,n)=(1,1)$  internal kink is revealed with a perfectly conducting wall placed at infinite

- ✓ The plot shows the perturbed velocity, radial component  $v^s(s)$ , of the **internal kink  $(m,n)=(1,1)$** .

$v^s(s)$  radial perturbed velocity of the **internal kink mode with no radial node**,  $\gamma\tau_A=0.023$  (rext=3.).

$v^s(s)$  radial perturbed velocity with **radial nodes**,  $\gamma\tau_A=0.0026$  (rext=3.).

- ✓ The growth rate decreases as the number of radial nodes increases.

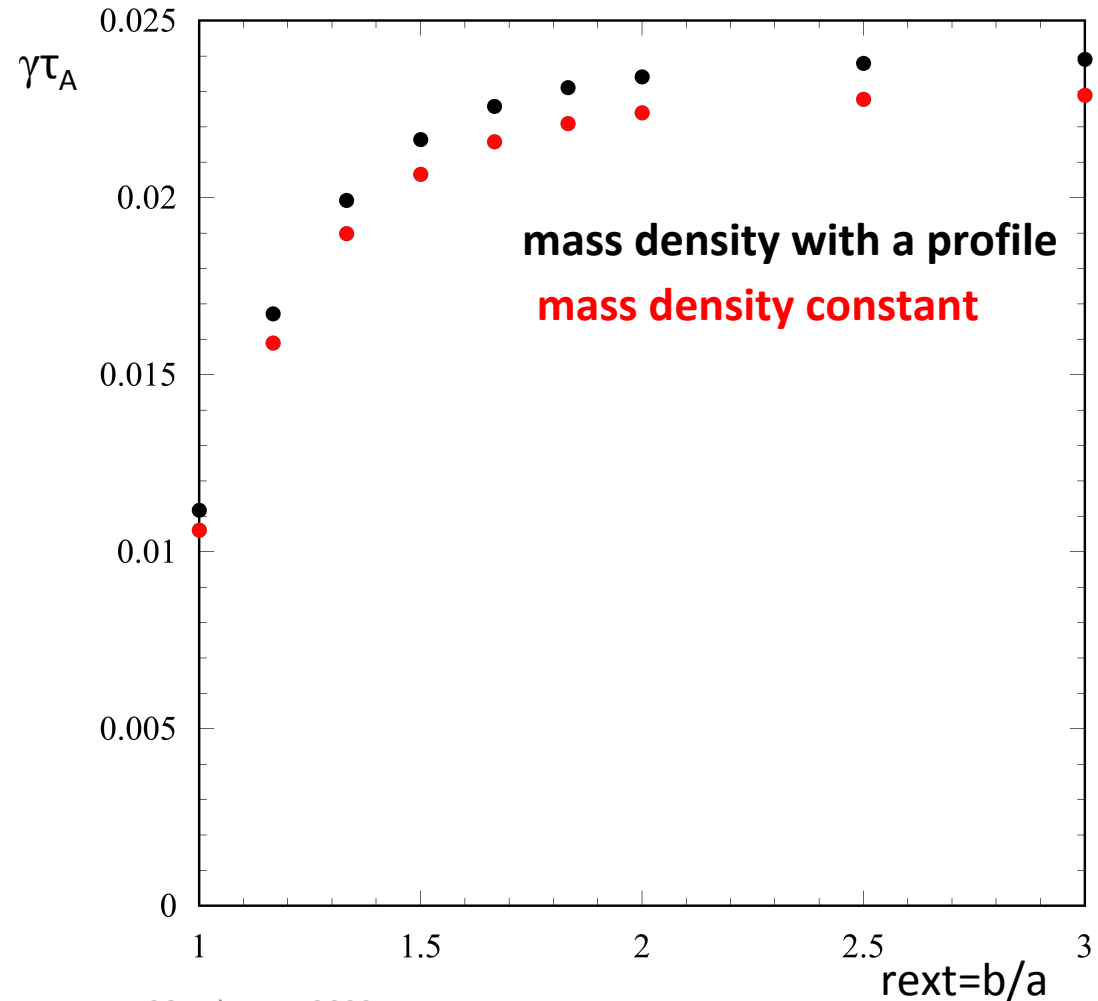


## Growth rate versus the wall position

- ✓ The mode growth rate has a dependence from the conducting wall position, meaning the mode contains an external mode component; anyway it survives when the perfect conducting wall is placed on the plasma surface that's why it is named "internal" kink.

- ✓ Moreover the plot shows that the difference, concerning the growth rate when a constant mass density is chosen, is negligible and the qualitative behaviour is the same.

- ✓ Thus, to simplify the analysis, a constant mass density profile has been chosen from here on.

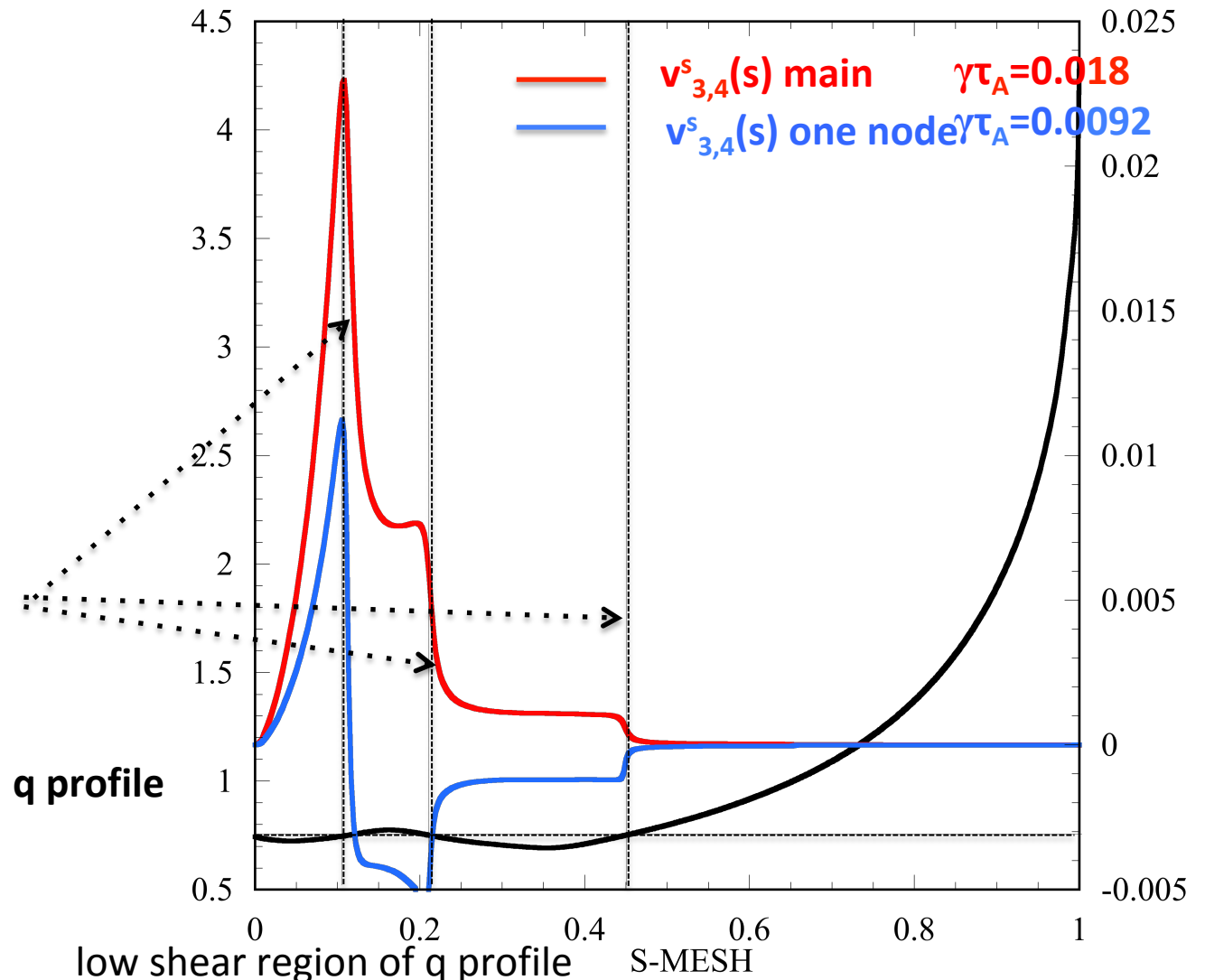


- ✓ No modes were found for  $n=2, 3, 5, 6, 9$  stability analysis
- ✓ Stability analysis for  $n=4, 7, 8, 10$  reveals the presence of **infernal modes** whose dominant mode numbers are  $(m,n)=(3,4), (5,7), (6,8), (7,10)$

As an example the perturbed radial velocity for modes number  **$(m,n)=(3,4)$**  is shown; in particular the **main infernal mode** with its **one node mode** is depicted. Note that the infernal multiple nodes modes have a lower growth rate with respect to the main mode.

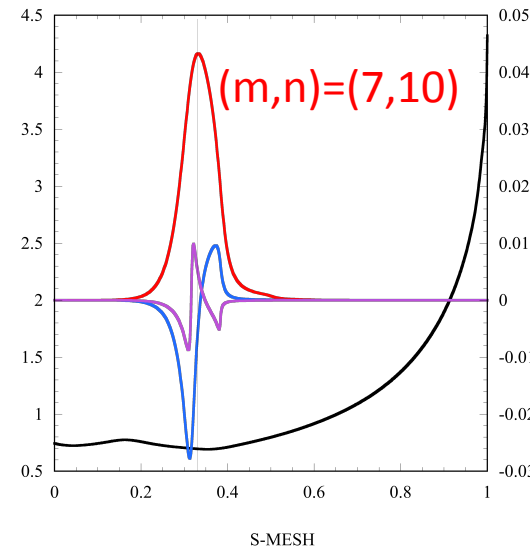
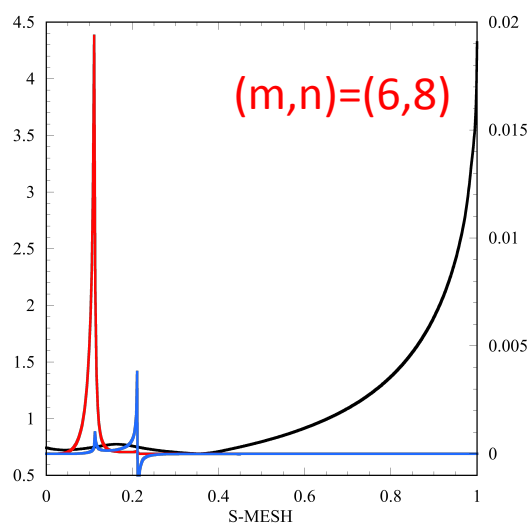
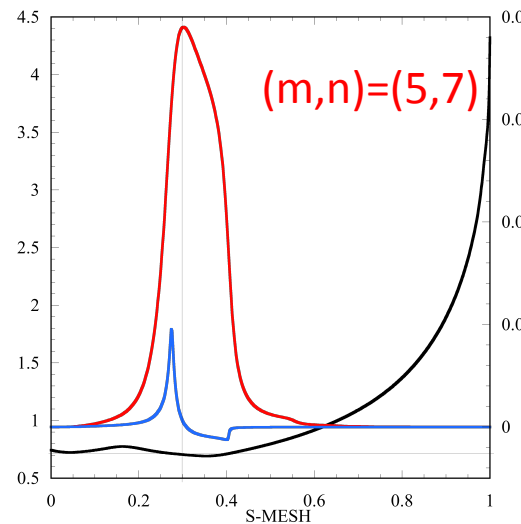
Note the presence of spikes or steps around the rational surfaces  $q=3/4$

$q=3/4=0.75 @ S\text{-MESH}=0.1$

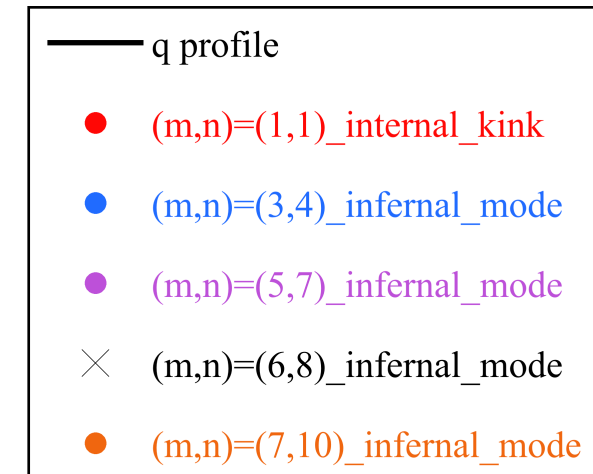
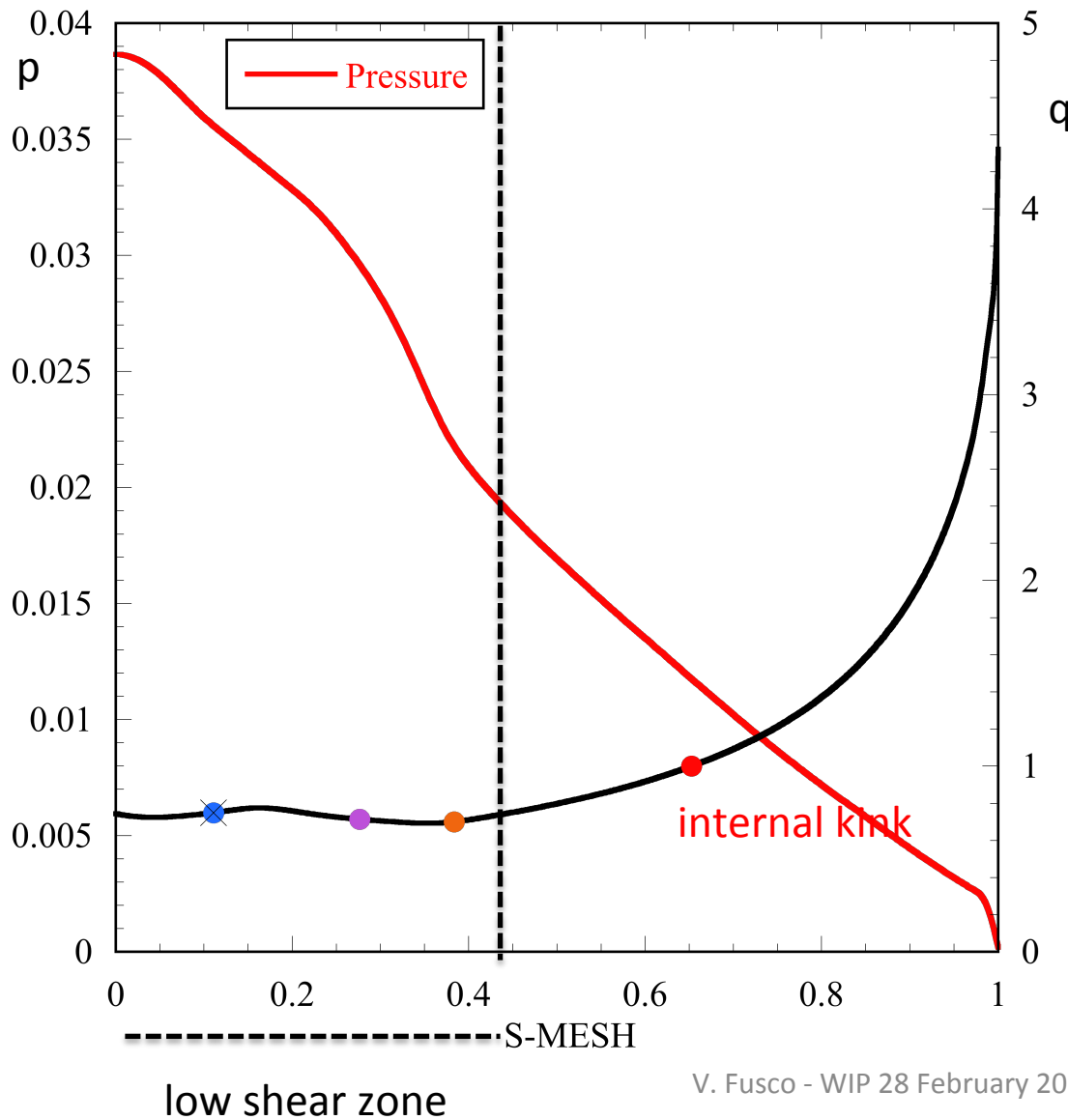


## Infernal modes for higher n

—  $v^s(s)$  main  
—  $v^s(s)$  one node  
—  $v^s(s)$  two nodes

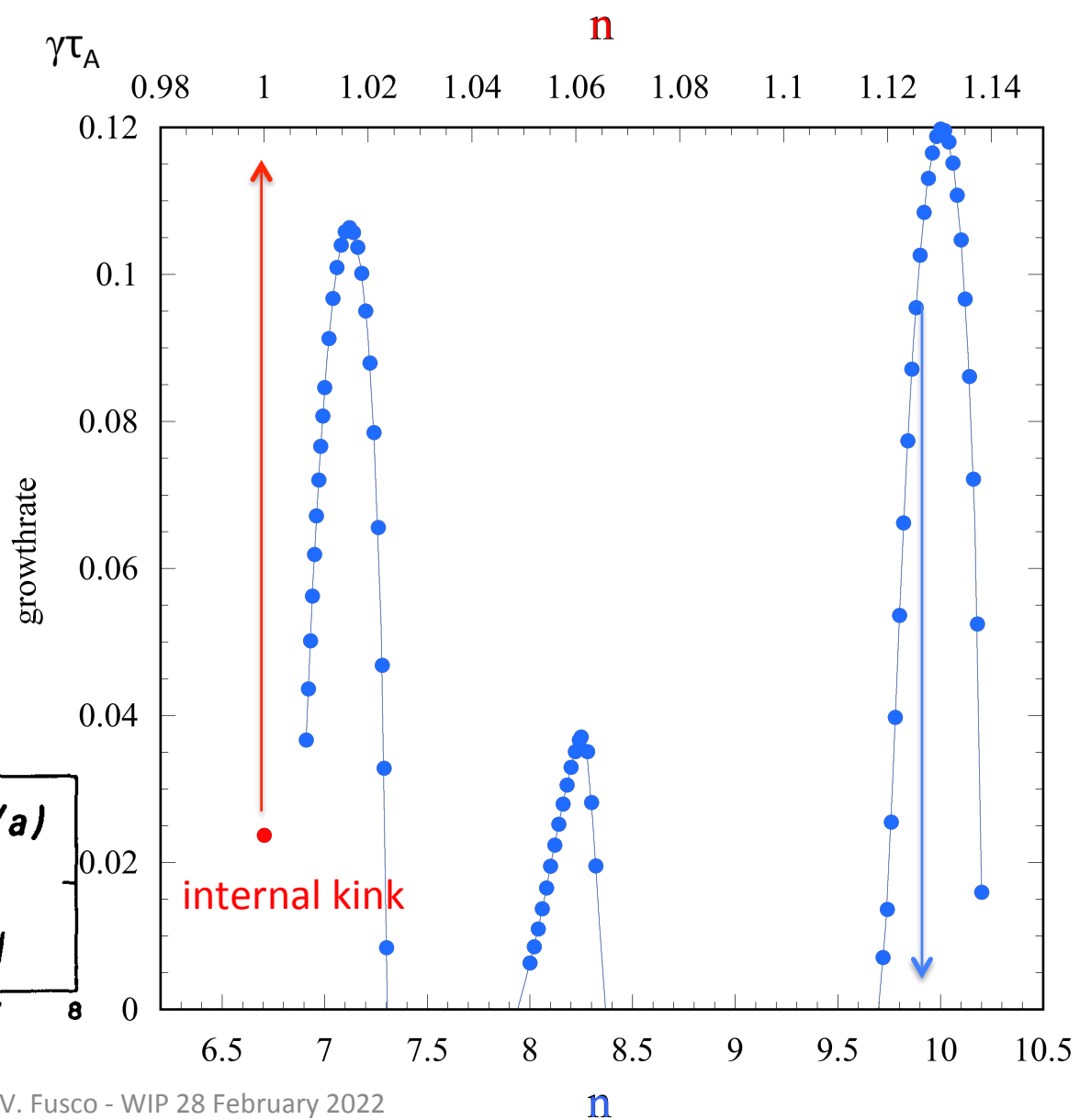
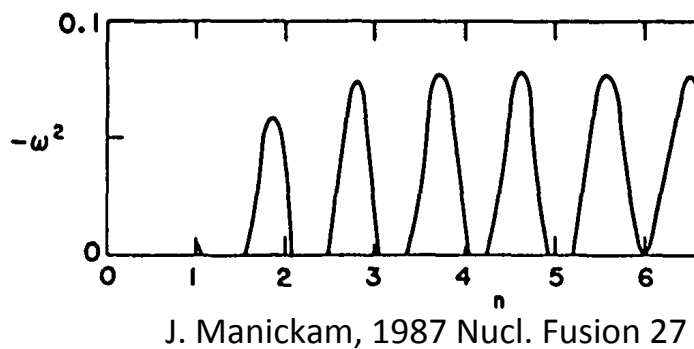


## Infernal modes position on q rational surfaces



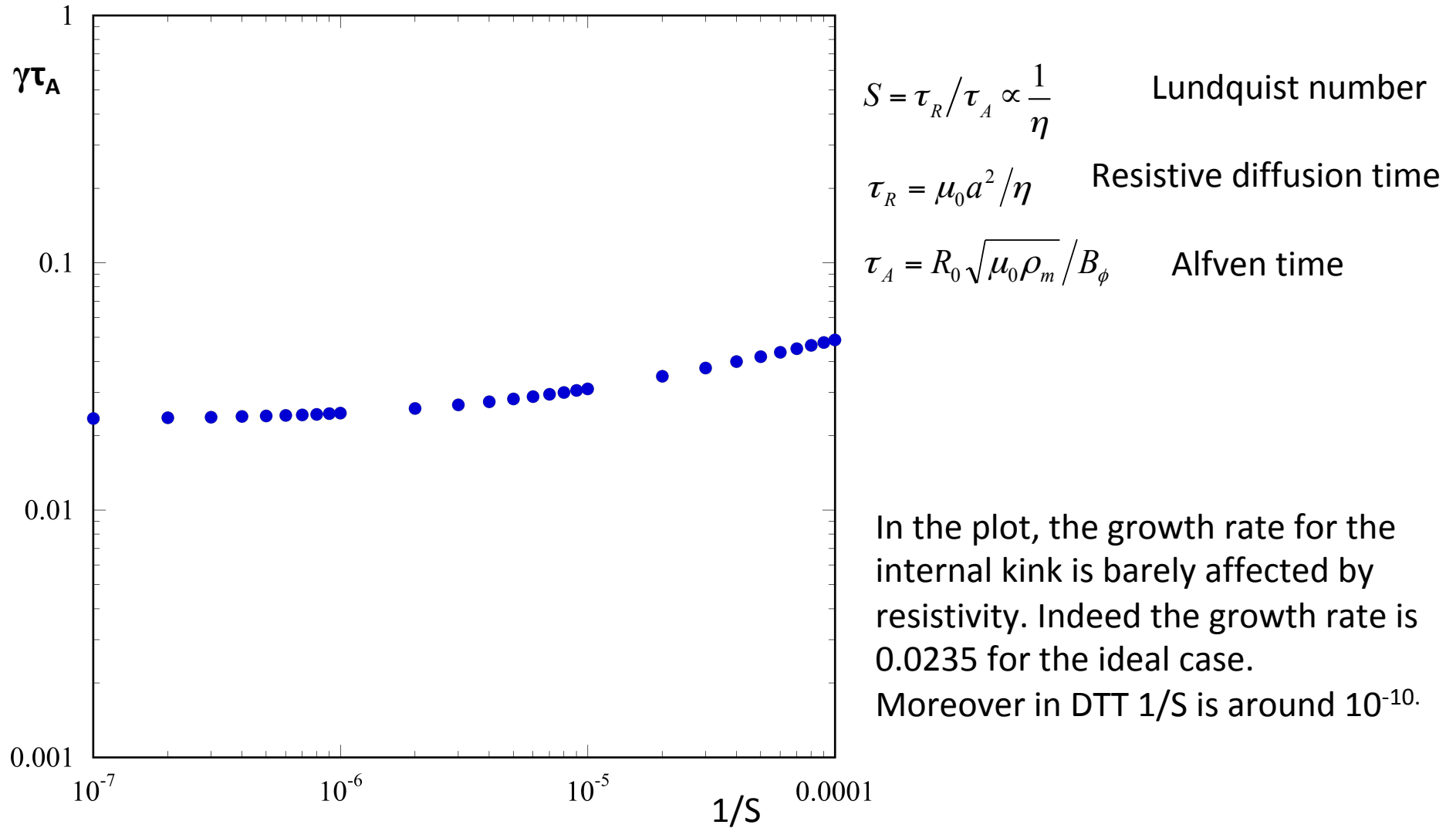
- ✓ The infernal mode is a **pressure driven** internal MHD instability, from low to intermediate toroidal n and poloidal m mode numbers, that is excited in a region of **low shear**.
- ✓ both conditions have to be simultaneously fulfilled. Indeed by setting  $p'=0$ , the mode disappears

- ✓ The plot shows the oscillatory behaviour of the internal mode growth rate with respect to  $n$  (as a continuous function); for this reason it is difficult to predict which  $n$  value is the most unstable. The same plot from Manickam analyses is shown [J. Manickam [5]]
- ✓ A red dot, which represents the internal kink growth rate, is reported for comparison.



## Stability analysis with MARS for the reference scenario: resistive study

- Resistive internal kink ( $m,n=(1,1)$ ) found. The plot shows the growth rate vs  $1/S$  for such mode.



- No tearing modes revealed. Mesh size densified around significant rational  $q$  surface to show modes in thin resistive layer.

## Sensitivity analysis varying i) $q_0 = q_{\text{axis}}$ and ii) $\beta_{\text{exp}}$

- ✓ Other quantities, such as total current  $I_t$ ,  $q_{\text{edge}}$ ..., profiles, are kept constant .



i)

	<b>ItotMA</b>	<b><math>q_0</math></b>	<b><math>q_{95\%}</math></b>	<b><math>q_{\text{edge}}</math></b>	<b><math>\beta_{\text{exp}}</math></b>	<b><math>\beta_N</math></b>
original	5.489	0.74	2.8450	4.3211	1.89	1.20
q_1	5.487	0.82	2.8747	4.0016	1.866	1.191
q_3	5.327	1.10	2.9072	3.999	1.803	1.328
q_3_bis	5.315	1.3	2.9636	4.0067	1.675	1.263
q_4	5.131	1.5	2.9965	4.0087	1.606	1.086

From CHEASE:  
 $\beta_* \% = 2.16493087$   
 $\beta_{\text{exp}} \% = 1.89007615$   
 $\beta_N = 1.20398$

ii)

	<b>ItotMA</b>	<b><math>q_0</math></b>	<b><math>q_{95\%}</math></b>	<b><math>q_{\text{edge}}</math></b>	<b><math>\beta_{\text{exp}} \%</math></b>	<b><math>\beta_N</math></b>
original	5.489	0.74	2.8450	4.3	1.89	1.20
0.5p0	5.505	0.75	2.82	4.2	0.0096	0.73
1.5p0	5.475	0.71	2.87	4.4	2.81	1.81
2p0	5.459	0.69	2.90	4.5	3.72	2.43
2.5p0	5.444	0.67	2.93	4.6	4.64	3.04

$$\beta_* \% = \frac{2\mu_0 (\langle p^2 \rangle)^{1/2}}{B_0^2}$$

$$\beta_{\text{exp}} \% = \frac{2\mu_0 \langle p \rangle}{B_0^2}$$

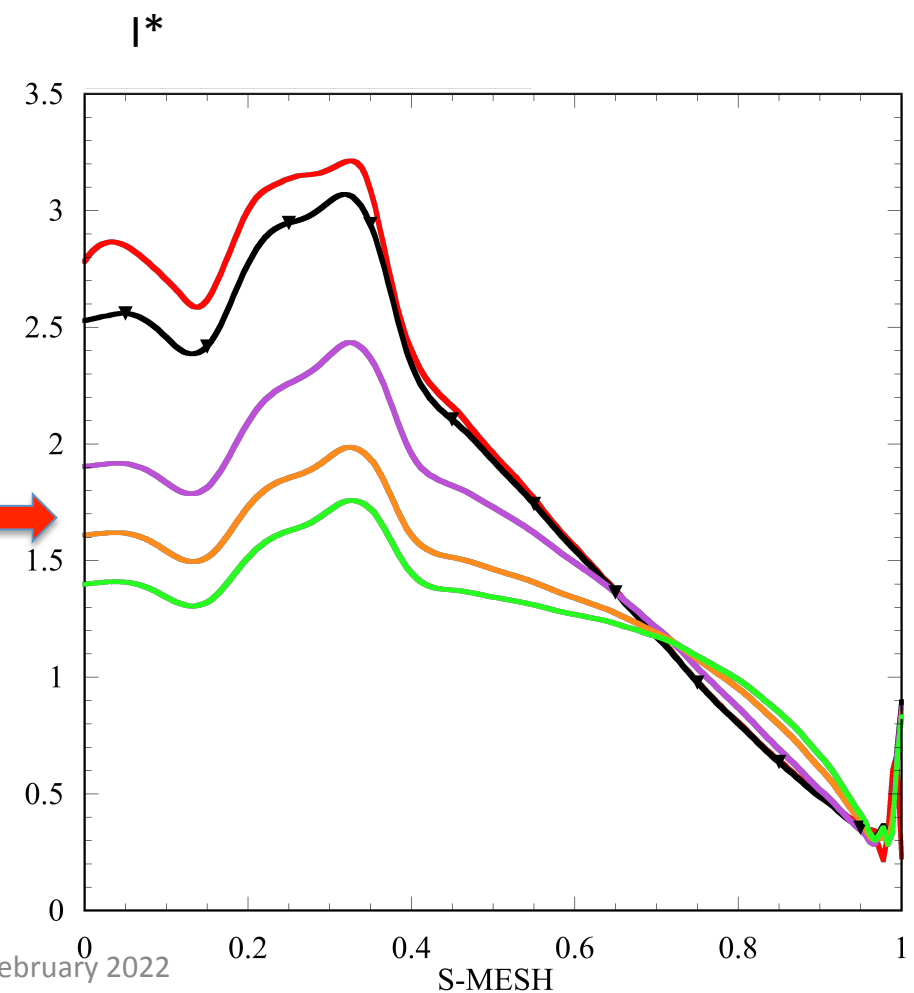
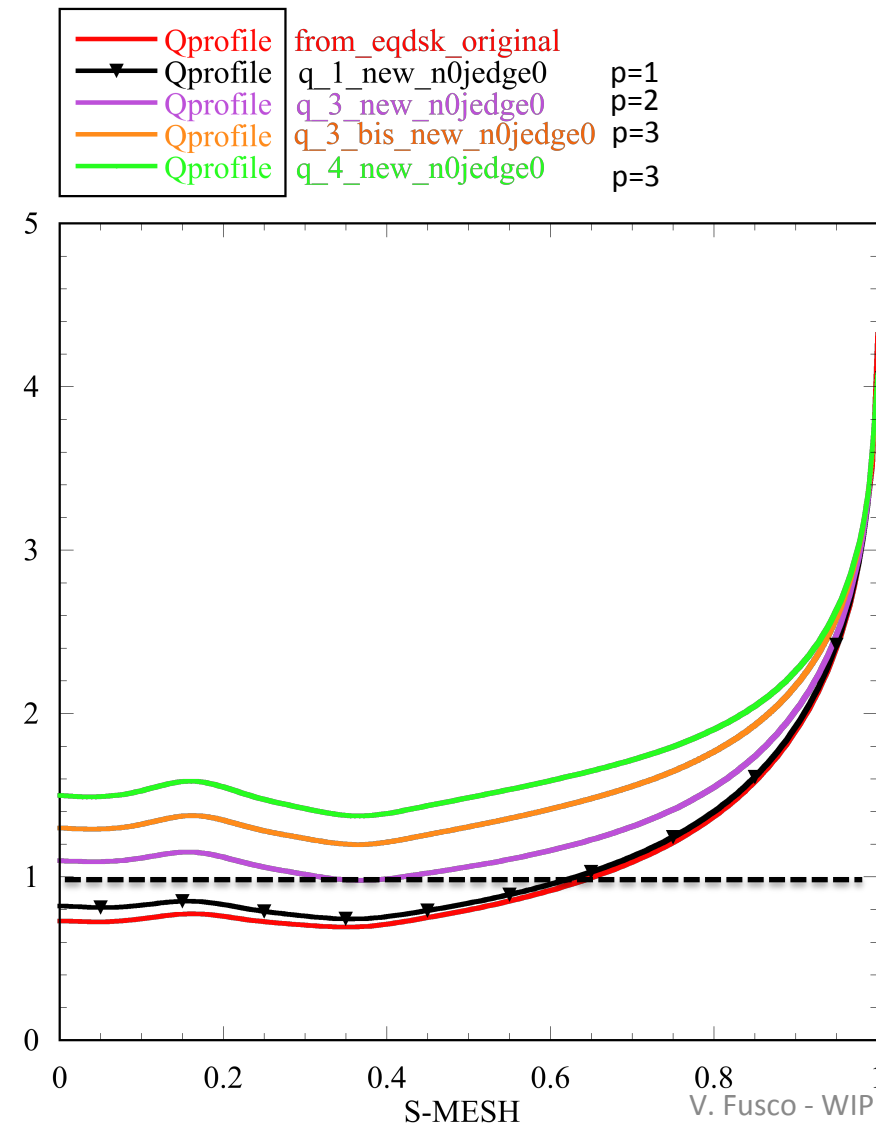
$$\beta_N = \frac{\beta_{\text{exp}} \%}{I_p / aB_0}$$

## i) Sensitivity analysis on $q_0=q_{\text{axis}}$

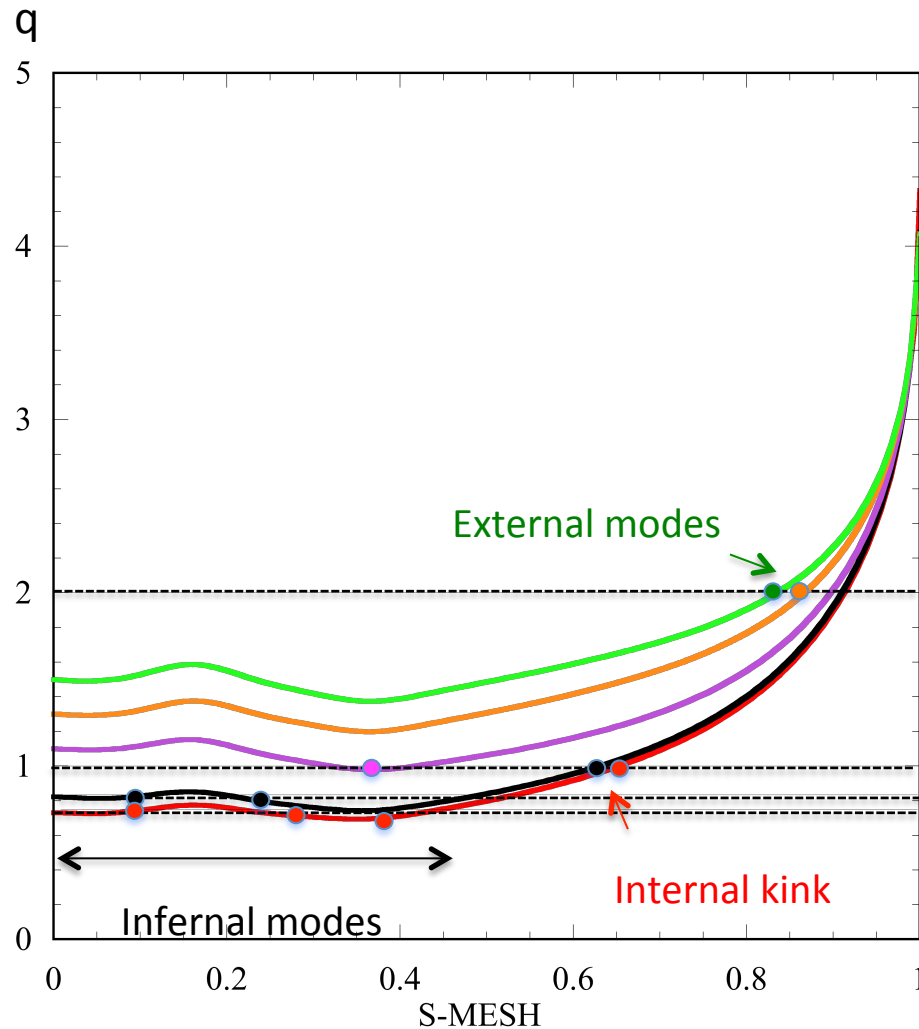
New analytical  $q$ , keeping the profile shape and the  $q_{\text{edge}}$  fixed:

$$q_{\text{new}}(s) = q(s) \left( 1 + k \left( e^{-s^p} - \frac{1}{e} \right) \right)$$

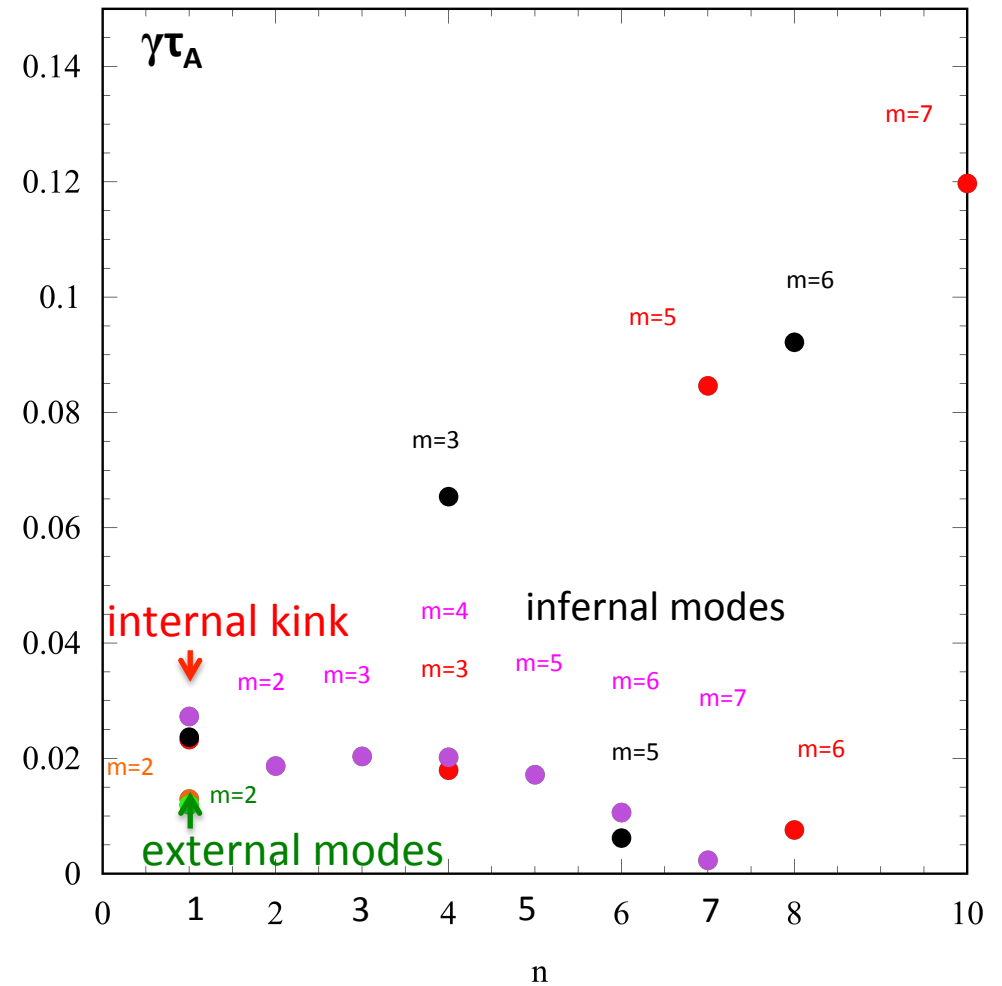
$$k = \left( \frac{q_{0\text{new}}}{q_0} - 1 \right) \frac{e}{e-1}$$



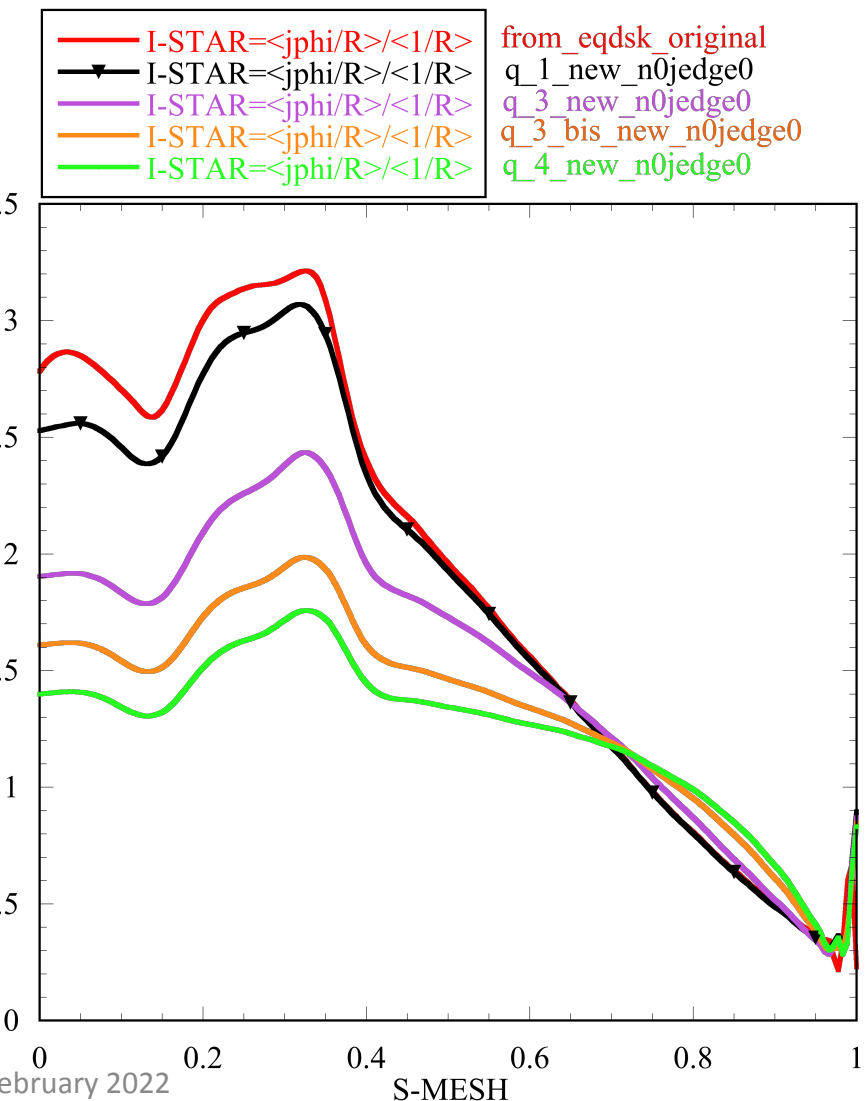
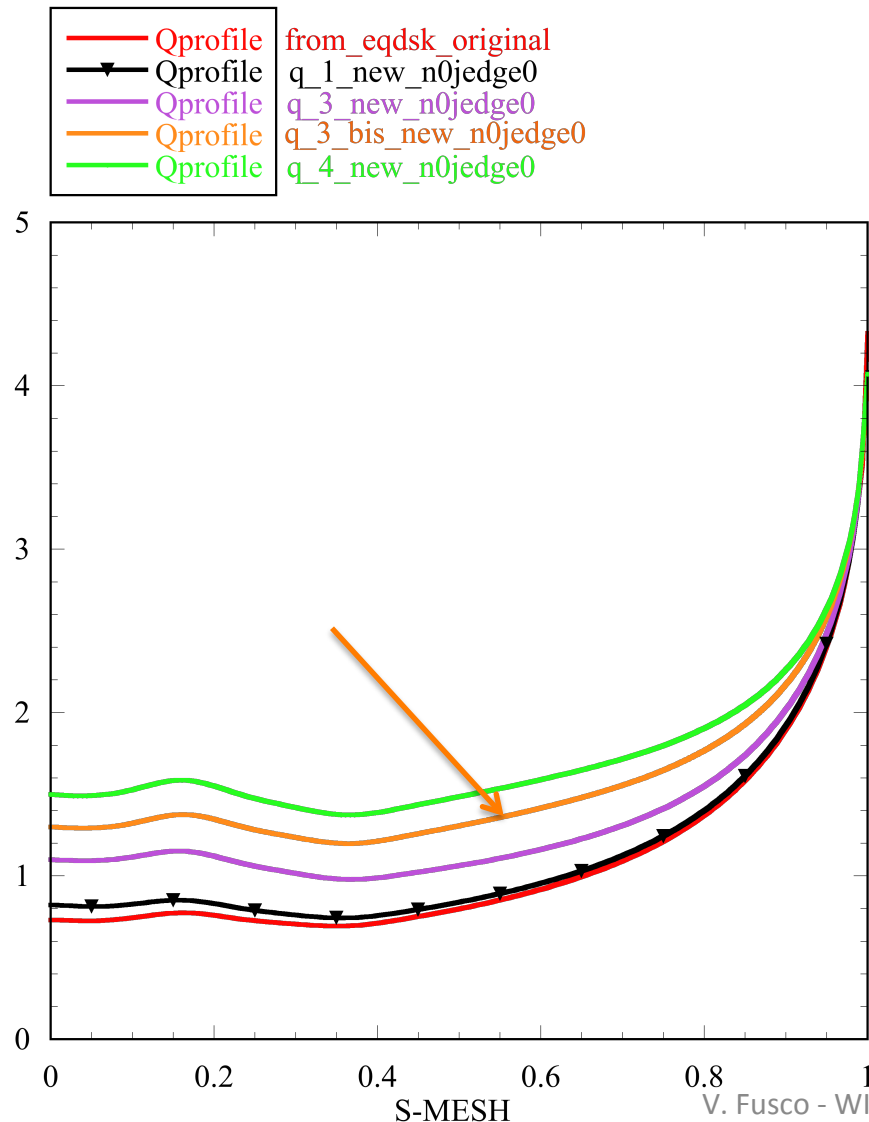
**Positions of the infernal modes, internal kink and external modes on the different safety factor q versus the s**



**Growth rate vs n**  
 $m$  are reported as well

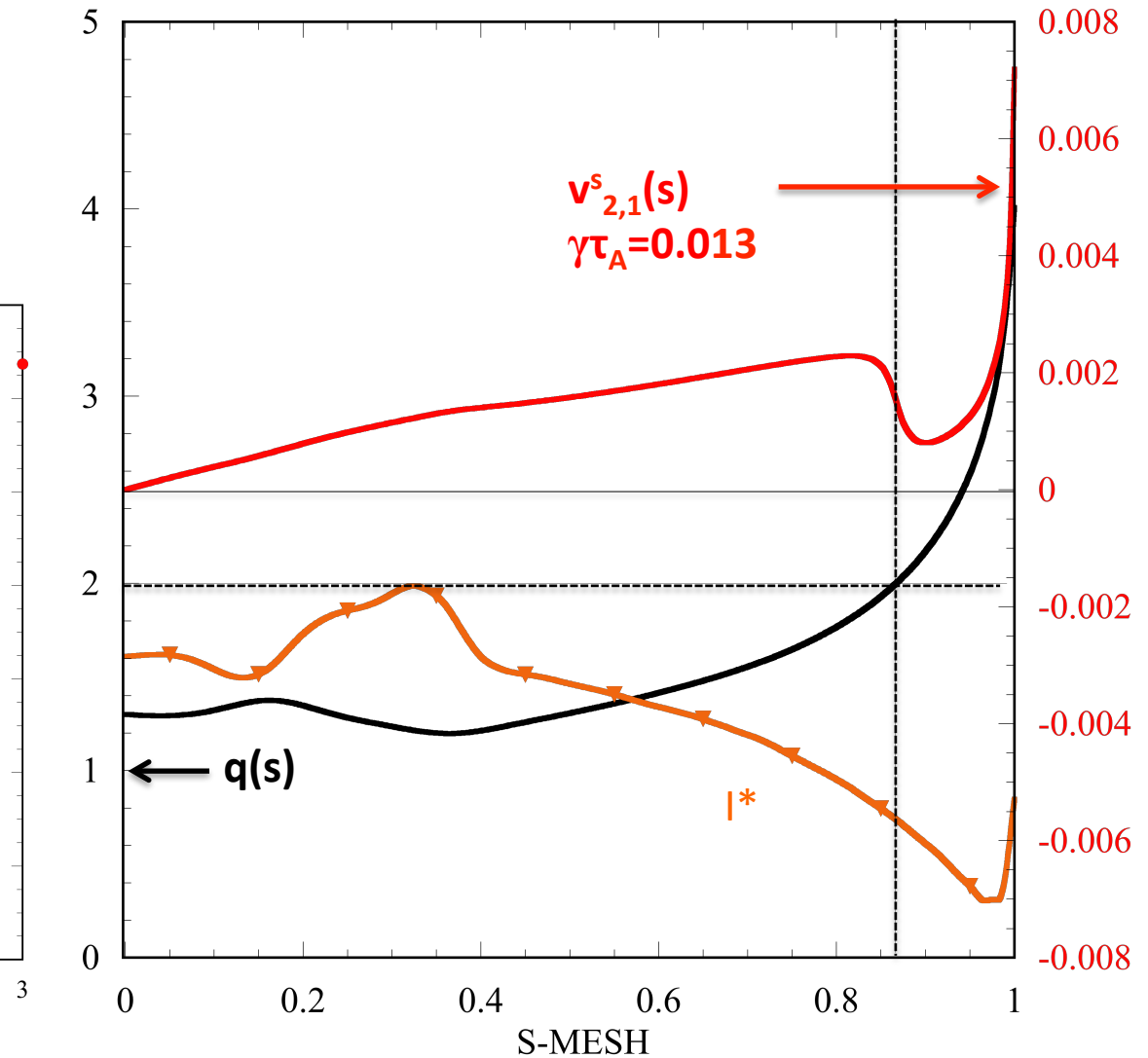
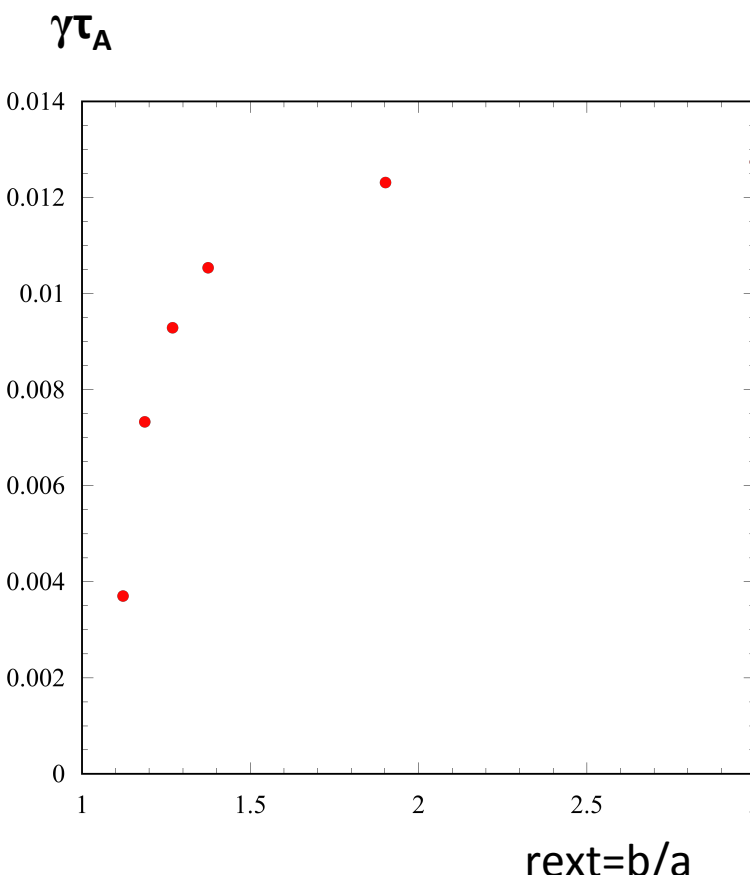


## MHD stability analysis $q_{\text{3\_bis}}$



No internal kinks, no infernal modes up to  $n=10$ .

- Only an  $m,n=2,1$  mode is revealed; it is an external mode as the following picture shows

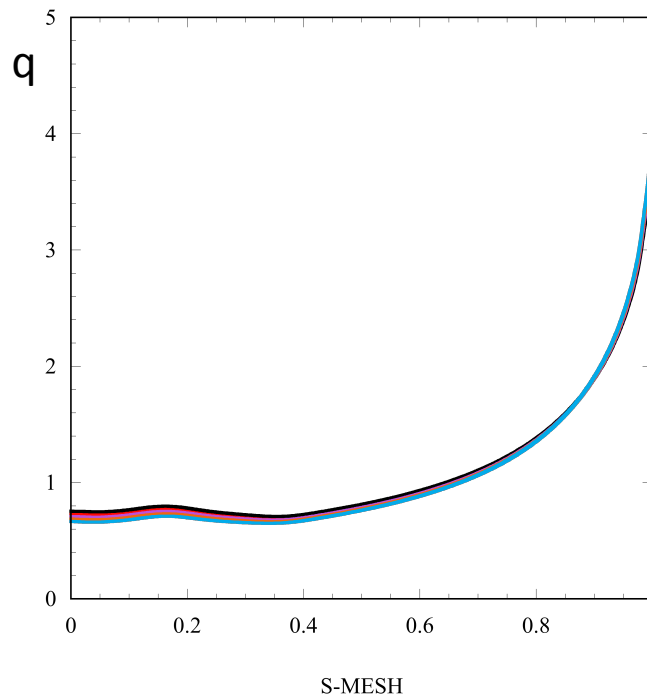


## Sensitivity analysis on ii) $\beta_{\text{exp}}$



		I <sub>totMA</sub>	q <sub>0</sub>	q <sub>95%</sub>	q <sub>edge</sub>	β <sub>exp</sub> %	β <sub>N</sub>
—	original	5.489	0.74	2.8450	4.3	1.89	1.20
—	0.5p0	5.505	0.75	2.82	4.2	0.0096	0.73
—	1.5p0	5.475	0.71	2.87	4.4	2.81	1.81
—	2p0	5.459	0.69	2.90	4.5	3.72	2.43
—	2.5p0	5.444	0.67	2.93	4.6	4.64	3.04

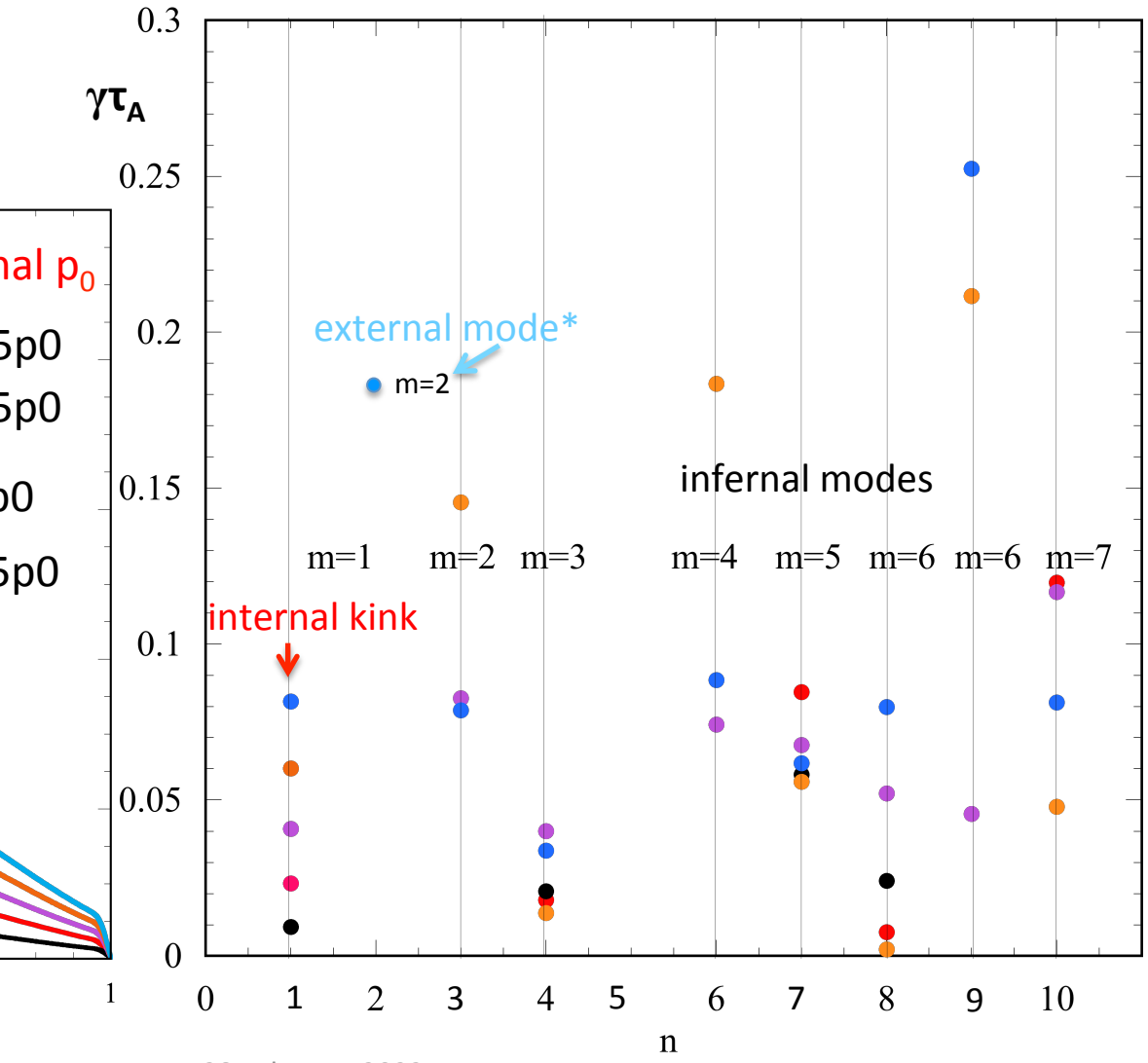
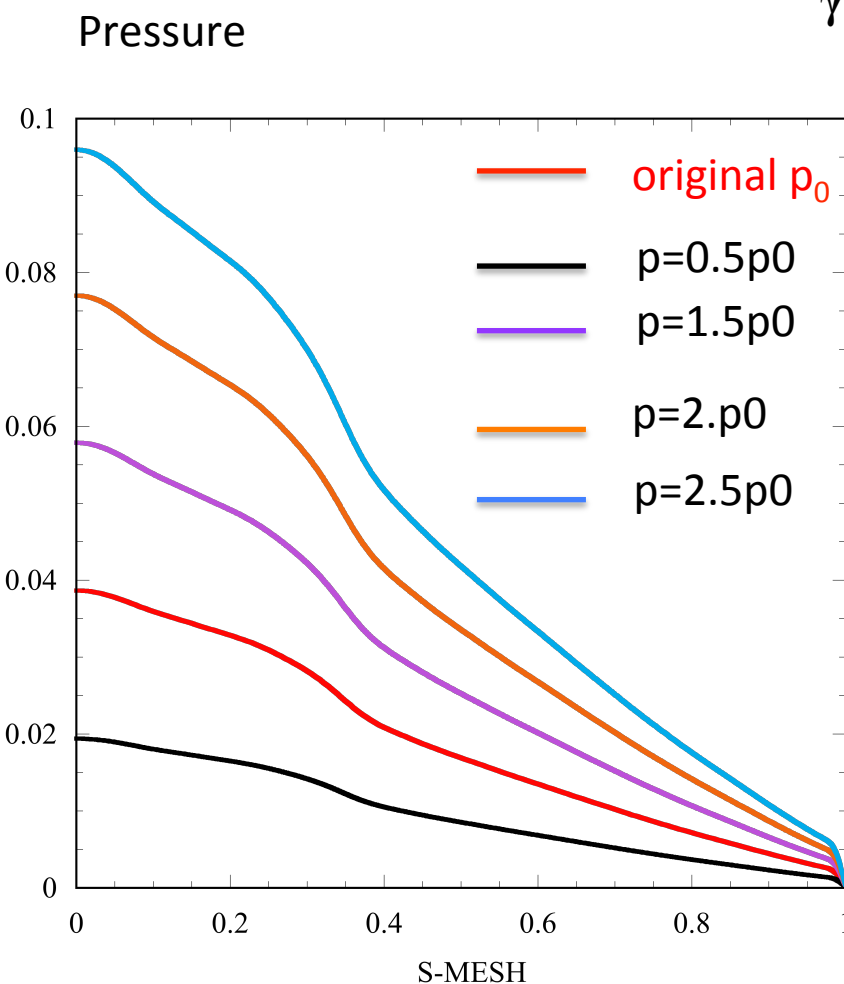
It results, as expected, very small changes on q profile...



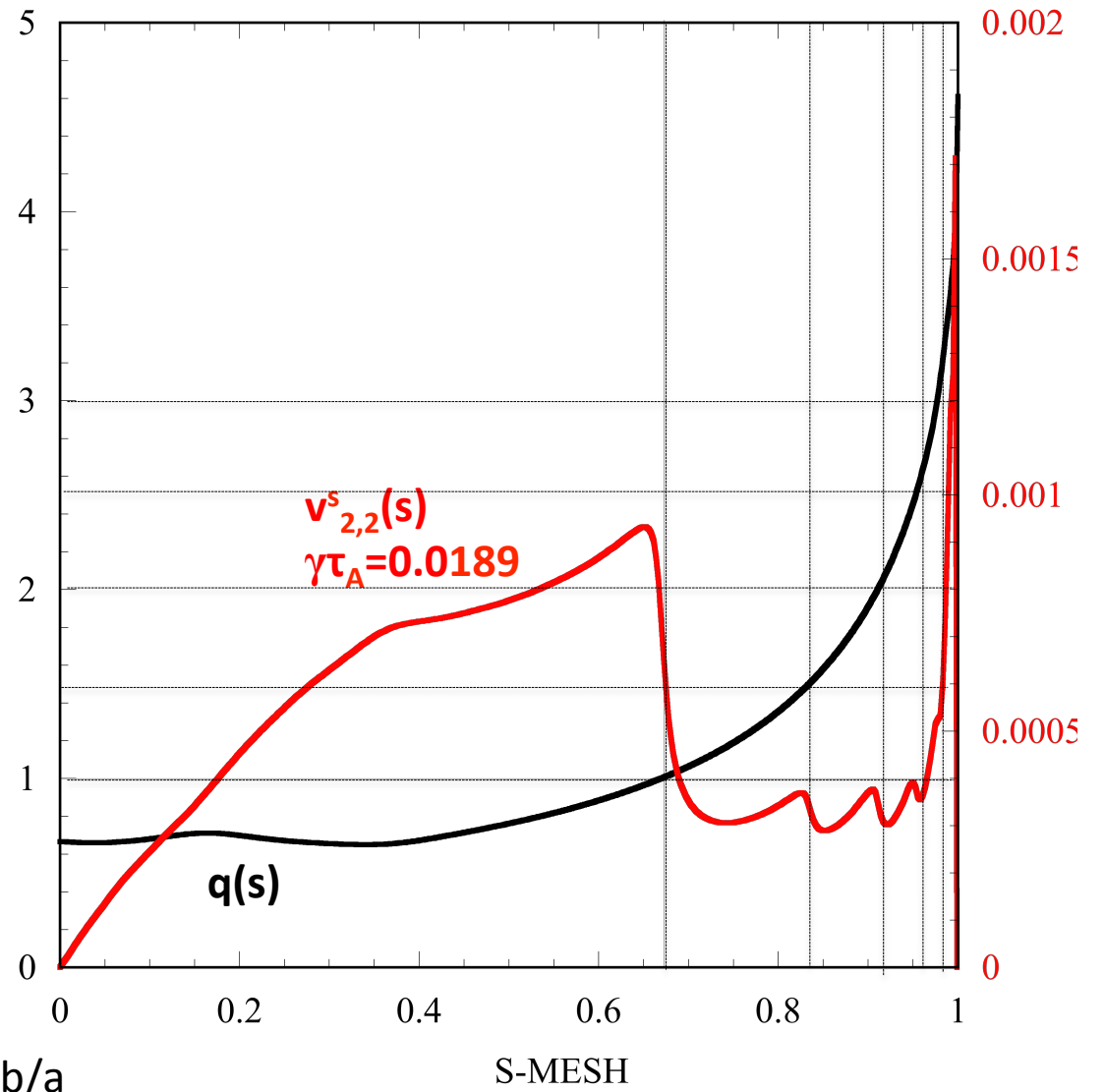
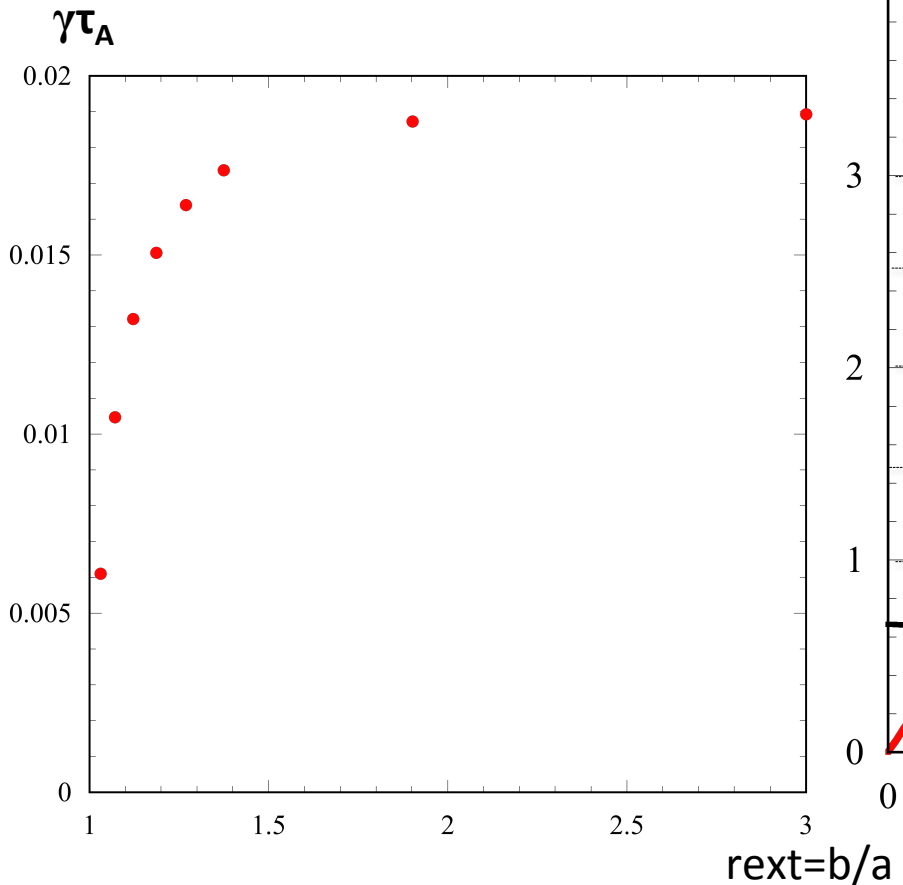
whilst the pressure changes...



As for the nominal case, internal kinks and infernal modes are revealed; the infernal modes position on  $q$  only slightly changes, because the  $q$  profile is almost untouched.



\*External mode  $m,n=2,2$



## Conclusions

- ✓ A stability analysis has been performed from low to intermediate toroidal mode number n
  - ✓ **for the reference scenario**

**Internal kink**  $(m,n)=(1,1)$  exists localized at a large radius

**Infernal modes** localized around the low shear and high gradient pressure zone are revealed. This analyses shows that such modes have higher growth rate than the internal kink, anyway the oscillatory behaviour of the growth rate with the mode number n makes it difficult to predict which n is the most unstable mode [6,7].

- ✓ **varying  $q_0$  and  $\beta_{\text{exp}}$**

An **internal kink**  $(m,n)=(1,1)$  does exist as long as  $q_0 \leq 1$

**Infernal modes** localized around the low shear and high gradient pressure zone are revealed. When  $q_0 > 1$  low-intermediate infernal modes disappear and  $(m,n)=(2,1)$  **external mode** appears.

When the  $\beta_{\text{exp}}\%$  is changed, q profile remains unperturbed thus the **internal kink**  $(m,n)=(1,1)$  is still unstable. **Infernal modes** are also revealed. As long as the pressure is increased  $(m,n)=(2,2)$  **external mode** appears.

- ✓ **Resistivity**, in this scenario, doesn't change the modes pictures

## Work in progress

- Characterization of low  $n$  MHD modes using **HYMAGYC** code (hybrid MHD –Gyrokinetic code developed in Frascati)
  - > towards adding kinetic effects
  - > use of the **FALCON** code (developed in Frascati) to characterize the Alfvén continua
- **JALPHA Workflow** has been already used to study the so called peeling-ballooning modes which are medium-to-high  $n$  ideal MHD modes, localized at the outermost plasma region. No modes were revealed. The equilibrium and stability codes used were HELENA and ILSA which are compatible with CHEASE and MARS; these codes uses a more convenient curvilinear geometry metrics thus they are prone to be inserted in the workflow.

## Bibliography

- [1] R. White, The theory of toroidally confined plasmas
- [2] G. Bateman, MHD Instabilities
- [3] H. Lütjens, A. Bondeson, O. Sauter, The CHEASE code for toroidal MHD equilibria, Computer Physics Communications, Volume 97, Issue 3, 1996, Pages 219-260,
- [4] A. Bondeson, G. Vlad, and H. Lütjens. Computation of resistive instabilities in toroidal plasmas. In IAEA Technical Committee Meeting on Advances in Simulations and Modelling of Thermonuclear Plasmas, Montreal, 1992, page 306, Vienna, Austria, 1993. International Atomic Energy Agency. Online version at  
<http://www.afs.enea.it/vlad/Papers/bondeson92iaeatcm.pdf>
- [5] J. Manickam et al 1987 Nucl. Fusion 27 1461
- [6] D. Brunetti et al 2016, Role of infernal modes dynamics and plasma rotation on the onset of NTMs in ECH-ECCD TCV plasmas J. Phys.: Conf. Ser. 775 012002
- [7] A. Kleiner et al., Nucl. Fusion 56 (2016) 092007
- [8] A.D. Turnbull et al 1988, Current and beta limitations for the TCV tokamak, Nucl. Fusion 28 1379
- [9] R.J. Buttery, DIII-D Research to Prepare for Steady State Advanced Tokamak Power Plants, Journal of Fusion Energy (2019) 38:72–111
- [10] A. Fasoli, Computational challenges in magnetic-confinement fusion physics, NATURE PHYSICS | VOL 12 | MAY 2016



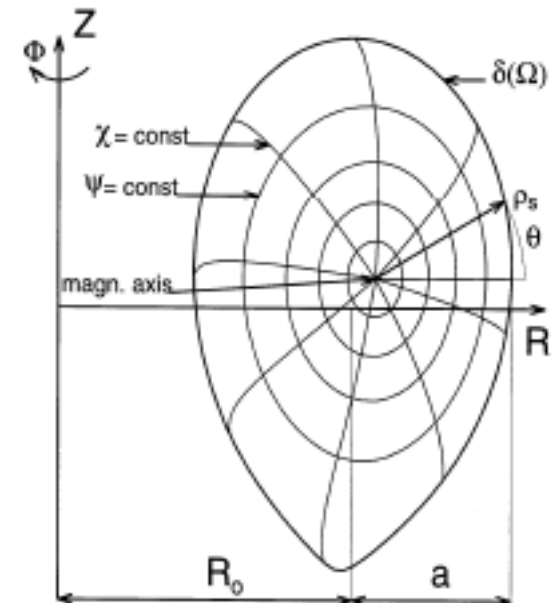
## CHEASE and MARS

The equilibrium code used is **CHEASE** [H. Lütjens, A. Bondeson, O. Sauter [3]], a **fixed boundary** code that solves the Grad-Shafranov equation **in toroidal geometry**, assuming static MHD equilibria and axisymmetry.

$$\nabla \cdot \frac{1}{R^2} \nabla \psi = \frac{j_\Phi}{R} = -p'(\psi) - \frac{1}{R^2} T T'(\psi)$$

Output relevant quantities

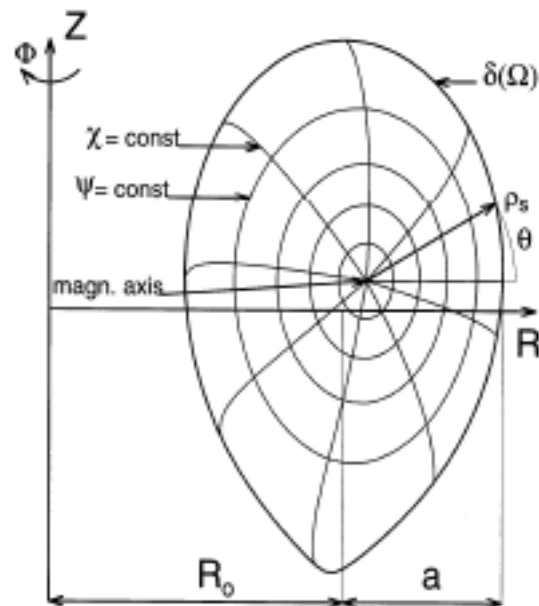
Poloidal flux  $\Psi$   
Metric tensor for different stability codes  
Equilibrium fields:  
•  $\underline{B} = T \nabla \phi + \nabla \phi \times \nabla \psi$



**cocos=2**  $\rightarrow (R, Z, \varphi), (\rho, \theta, \varphi)$

# MARS

- **Resistive** spectral code for full MHD **linear** stability analysis
- Two dimensional, **axisymmetric** general **toroidal** geometry carried out in **flux coordinate**  $(s, \chi, \phi)$   
where  
 $s = (1 - \psi/\psi_{\text{axis}})^{1/2}$  is the radial-like coordinate,  
 $\psi$  is the poloidal flux function  
 $\chi$  is a **generalized poloidal angle** which depends on the choice for the Jacobian\*  
 $\phi$  is the geometrical toroidal angle.



$$* J = C(\Psi) R^{\text{NEGP}} |\text{grad} \Psi|^{\text{NER}}$$

$$\chi(\theta) = \int_0^\theta \frac{R \sigma \rho_s^2(\tilde{\theta})}{J \partial \Psi / \partial \sigma} d\tilde{\theta}$$

NER = 2	NEGP = 0	$J_\psi \propto R^2$	⇒ "Princeton Jacobian"
NER = 0	NEGP = 0	$J_\psi \propto \text{Constant}$	⇒ "Hamada Jacobian"
NER = 1	NEGP = -1	$J_\psi \propto R/ \nabla \psi $	⇒ "Equal arc length Jacobian"

The choice of the Jacobian have consequences on the  $\chi$  mesh:

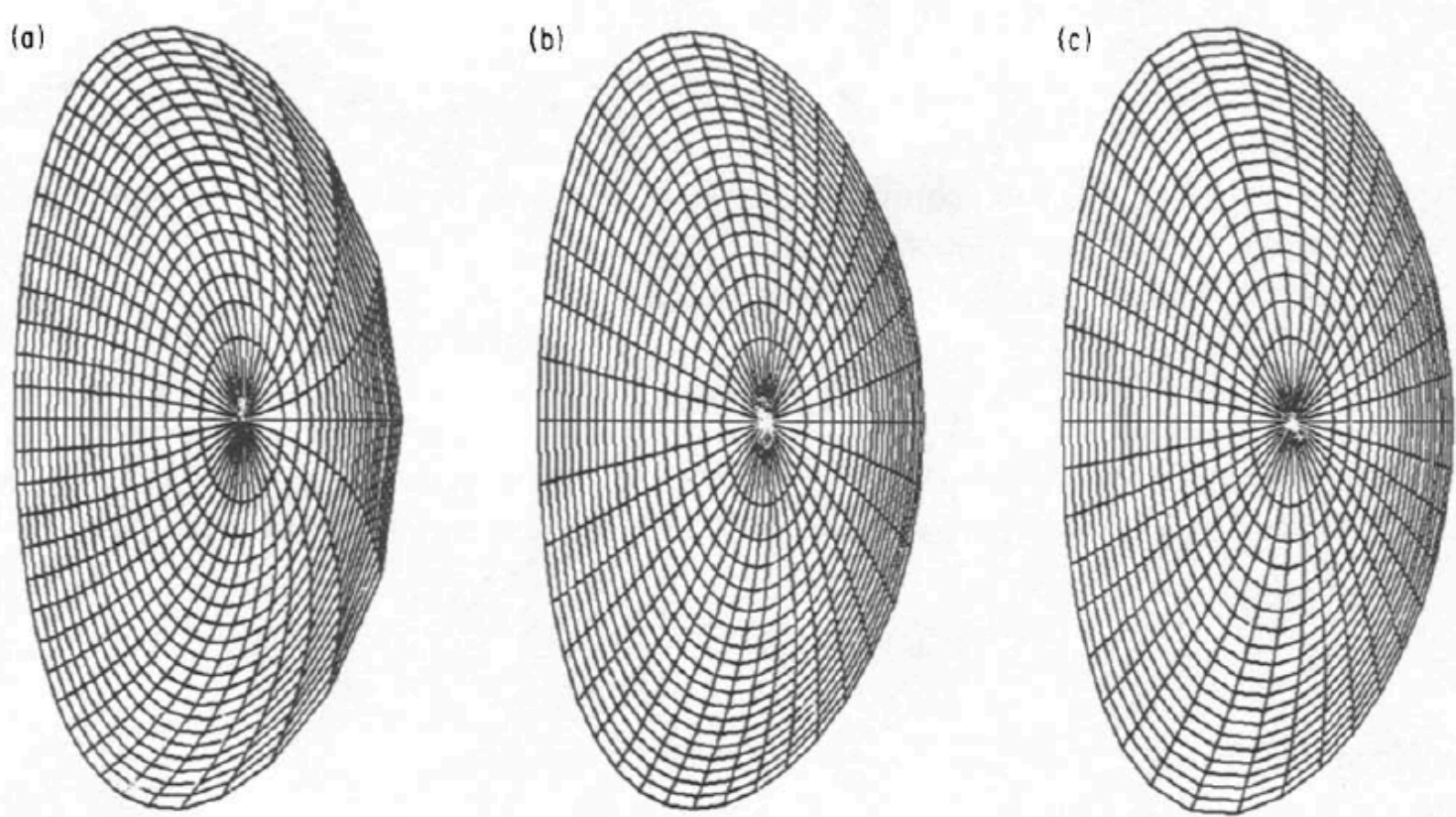


FIG. 2. Equally spaced  $(\psi, \theta)$  meshes for (a) PEST, (b) Hamada, and (c) equal arc length coordinate system for the equilibrium of Eq. (27) with  $R = 1$ ,  $E = 1/2$ ,  $q = 1.2$ ,  $q_{\text{edge}} = 2.1$ .

The equilibrium fields ( $B^\chi, B^\phi$ ), currents ( $J^\chi, J^\phi$ ) and the covariant metric tensor ( $g_{ij}$ ) are supplied in Fourier representation by the equilibrium code Chease

The perturbations of velocity, magnetic fields and current density are represented as

$$\underline{v} = J(v^s \nabla \chi \times \nabla \phi + v^x \nabla \phi \times \nabla s + v^\phi \nabla s \times \nabla \chi)$$

$$\underline{b} = b^s \nabla \chi \times \nabla \phi + b^x \nabla \phi \times \nabla s + b^\phi \nabla s \times \nabla \chi$$

$$\underline{j} = j^s \nabla \chi \times \nabla \phi + j^x \nabla \phi \times \nabla s + j^\phi \nabla s \times \nabla \chi$$

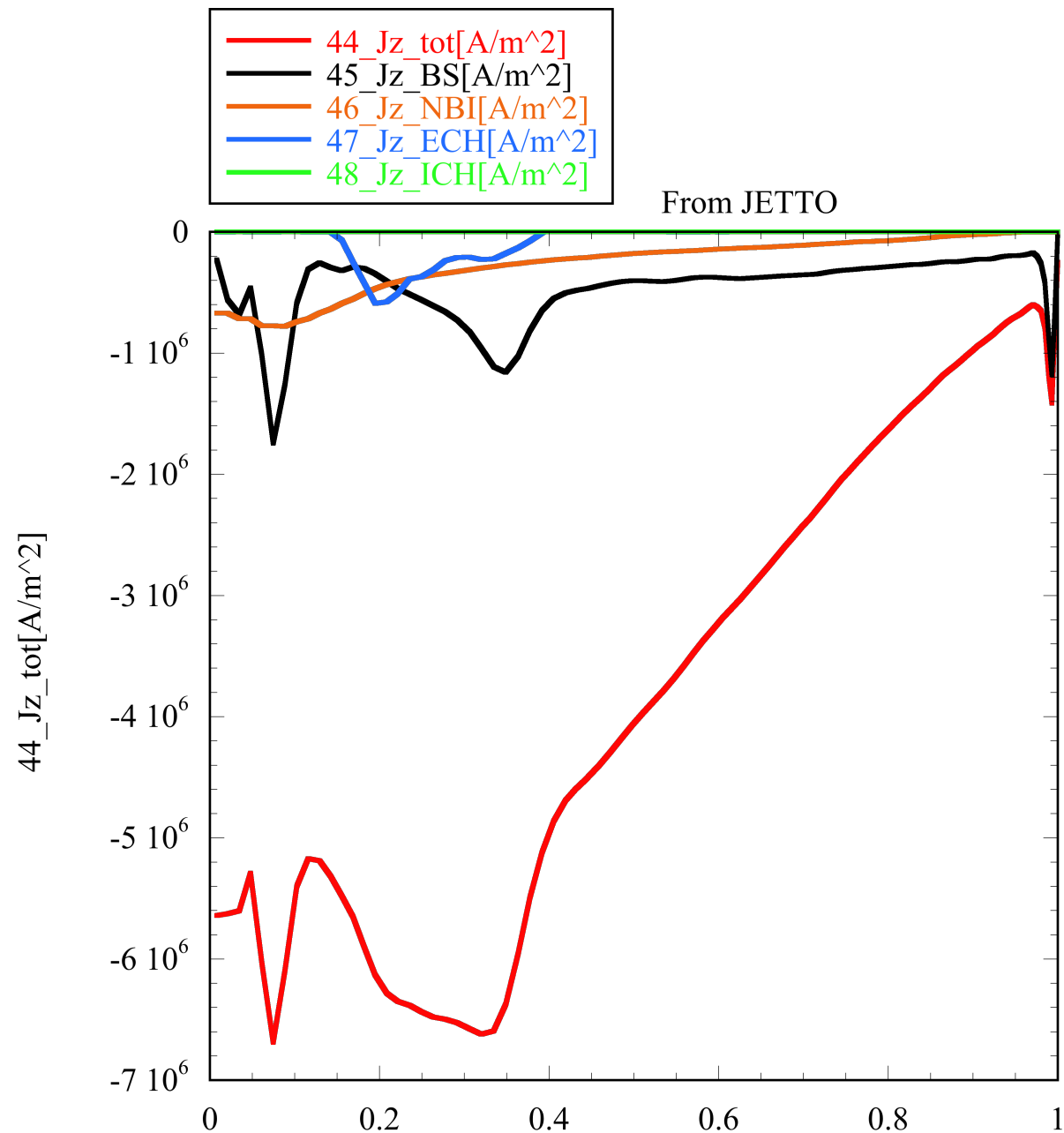
MARS decomposes in Fourier the poloidal and toroidal angular variation:

$$v^s(s, \chi, \phi) = e^{in\phi} \sum_{m=m_1}^{m_2} v_m^s(s) e^{im\chi} \quad v^\chi(s, \chi, \phi) = e^{in\phi} \sum_{m=m_1}^{m_2} v_m^\chi(s) e^{im\chi} \quad v^\phi(s, \chi, \phi) = e^{in\phi} \sum_{m=m_1}^{m_2} v_m^\phi(s) e^{im\chi}$$

$$b^s(s, \chi, \phi) = e^{in\phi} \sum_{m=m_1}^{m_2} b_m^s(s) e^{im\chi} \quad \dots$$

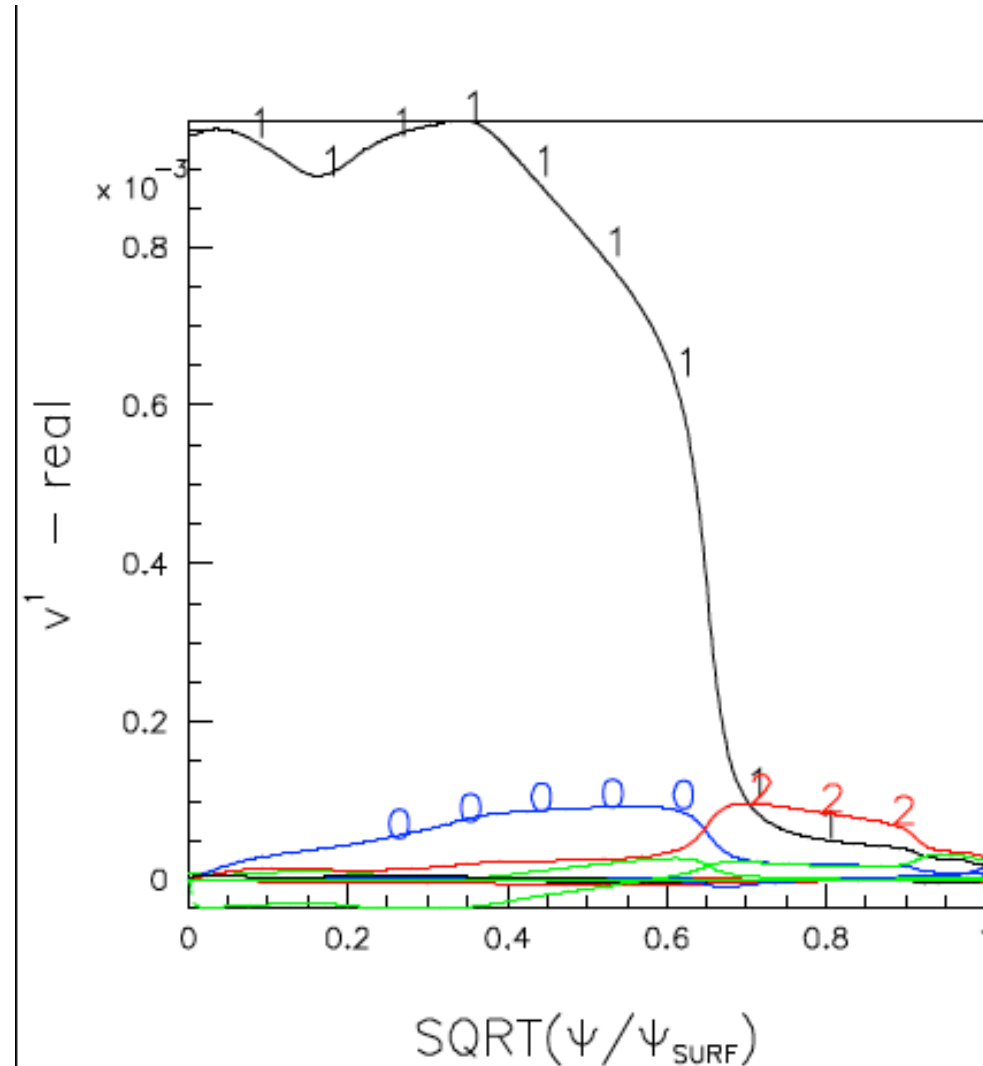
...

The discretization in  $s$  uses the **finite element method** (FEM) piecewise linear and piecewise constant (integer grid and half grid respectively).

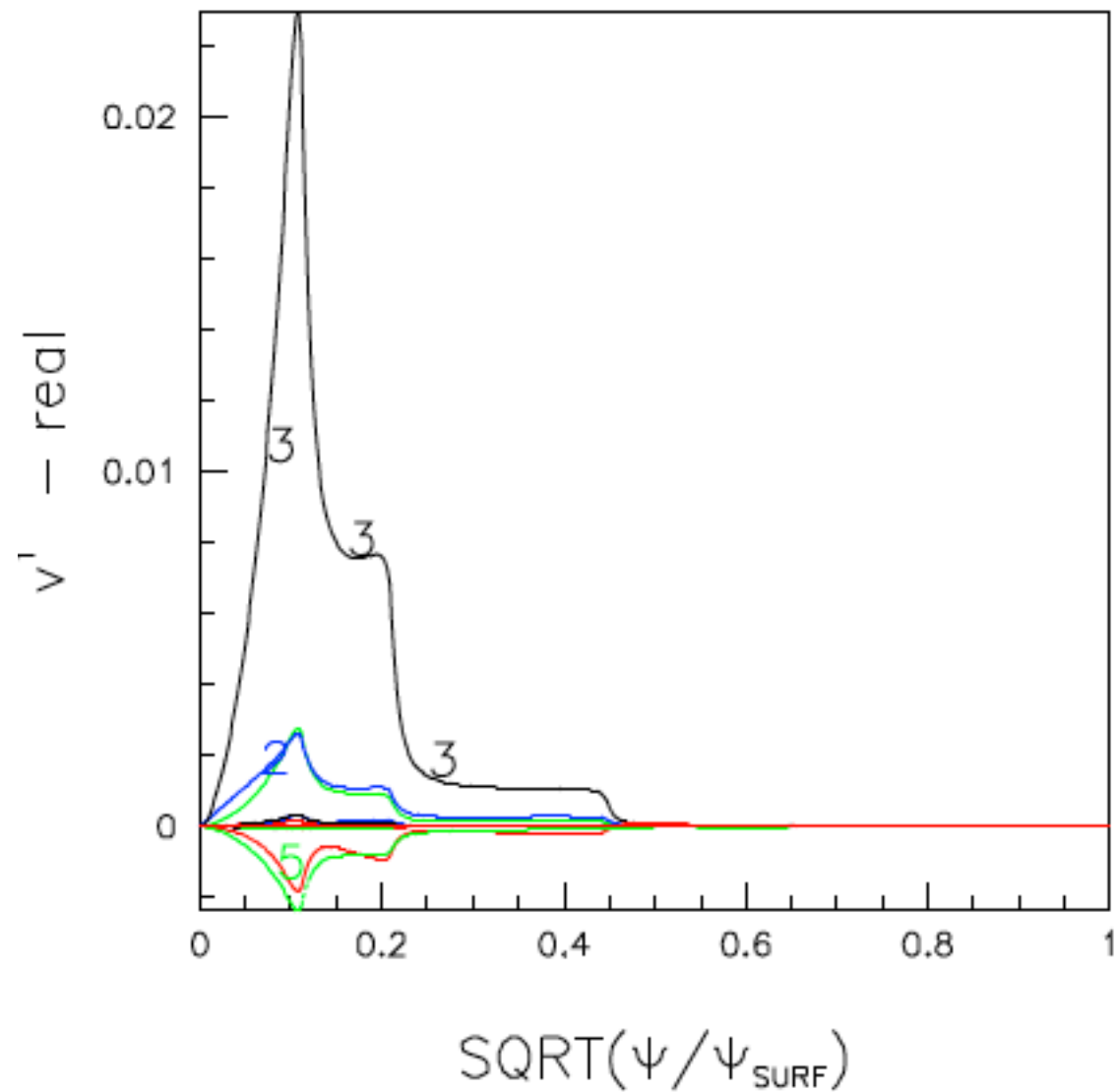


Reference scenario

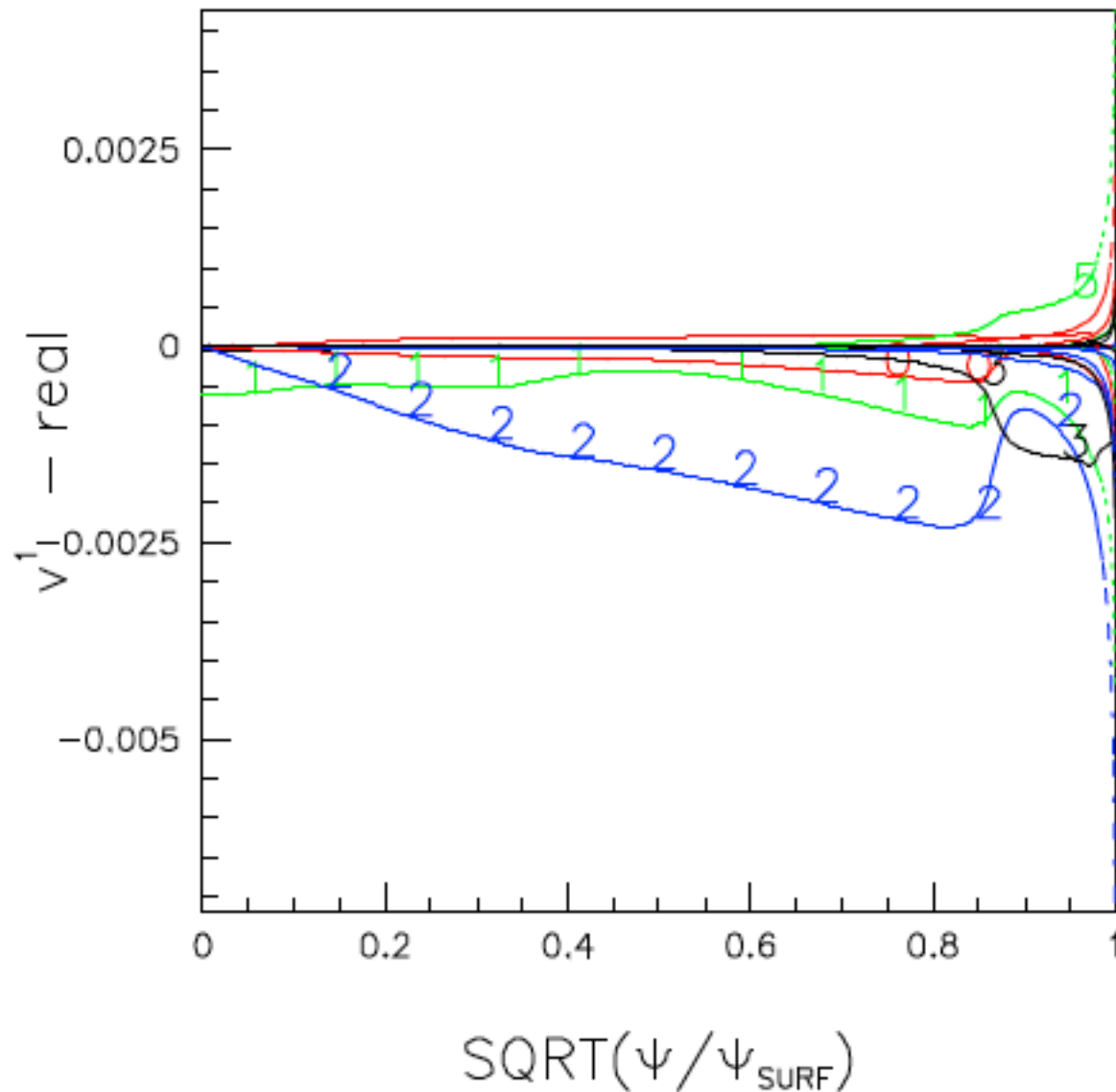
Internal kink  $(m,n)=(1,1)$  with the others  $m$  components



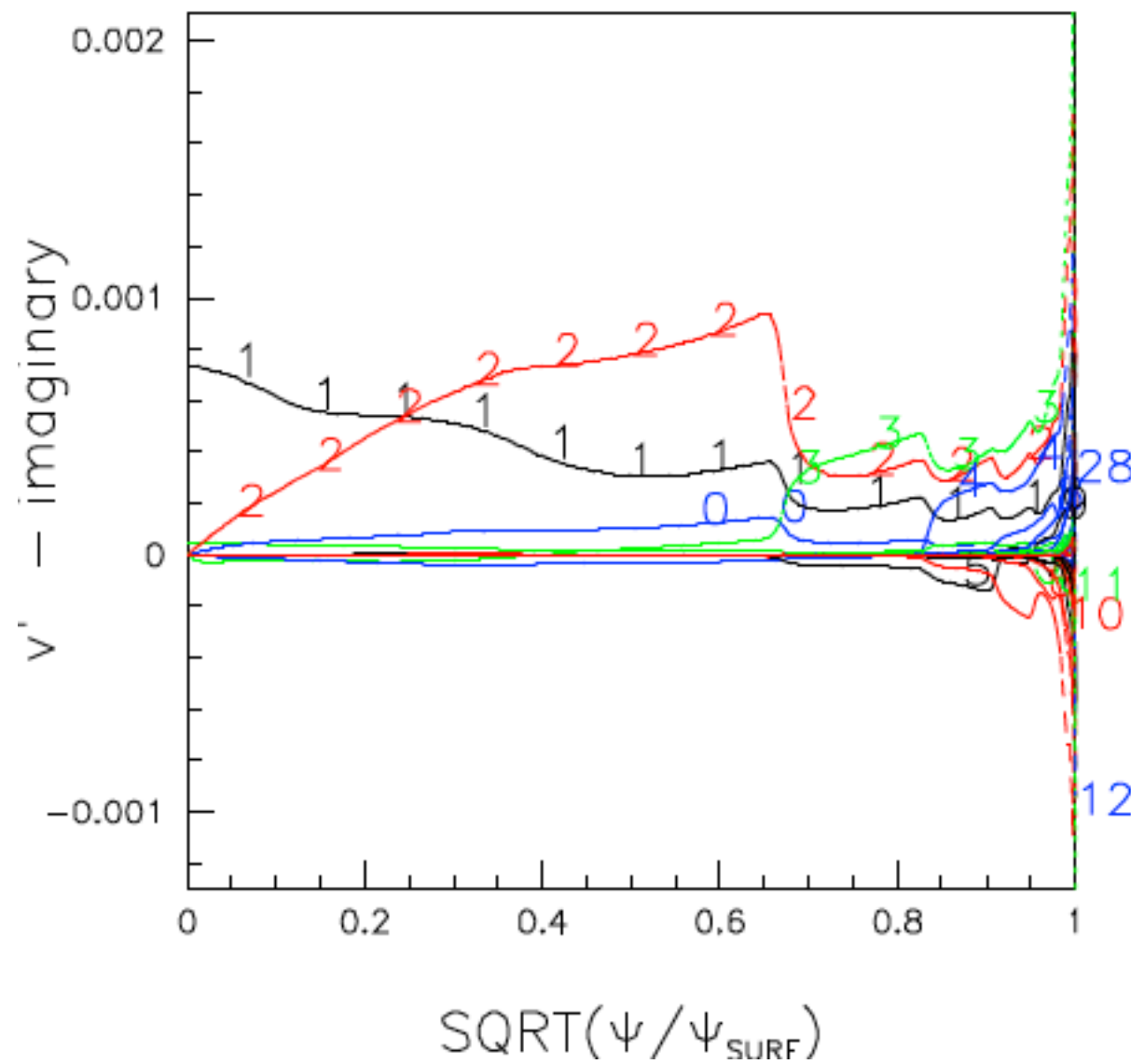
Infernal Mode m,n=3,4



## External mode m,n=2,1 q\_3\_bis



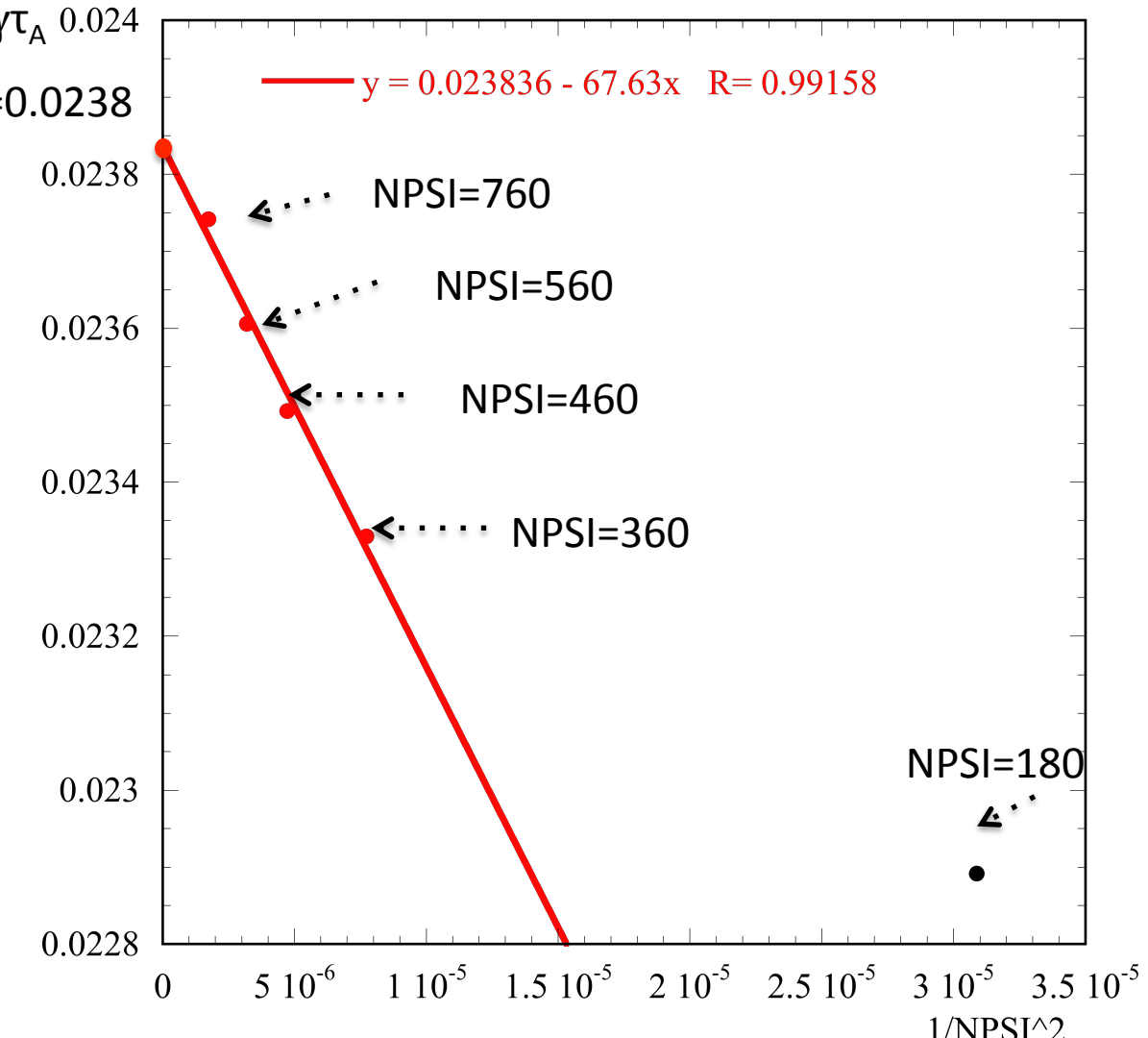
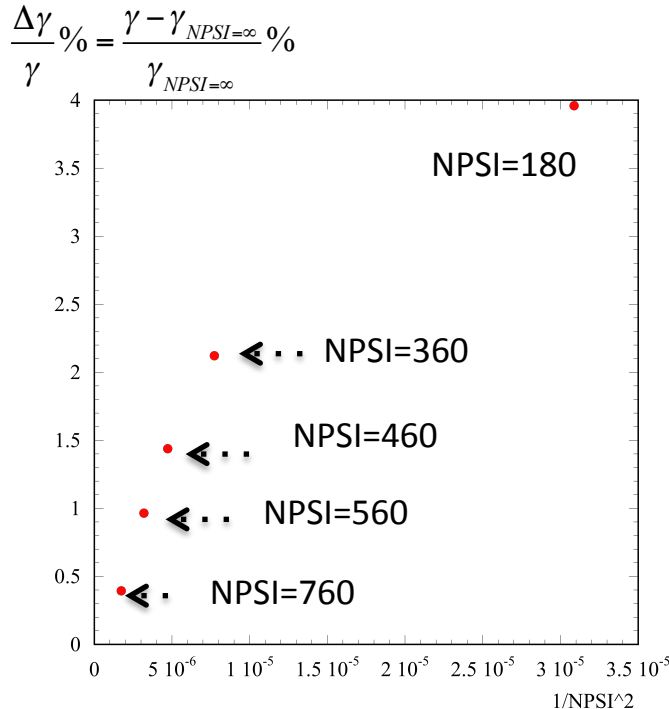
External m,n=2,2 p=2.5p0



## Convergences test: mesh size

MARS results has been validated with convergences tests

- The eigenvalue converges quadratically with the mesh size:  $\Delta\gamma = 1/NPSI$
- When  $NPSI=360$  (mesh size in  $\psi$ ), the error is within %.



## MARS sensitivity studies: spectral components

Sensitivity analysis on the spectral component  $m_1, m_2$  for  $n=1$

$$v^s(s, \chi, \phi) = e^{in\phi} \sum_{m=m_1}^{m_2} v_m^s(s) e^{im\chi}$$

...

- NPSI=360
- NPSI=460

In these simulations  $m_1=-5$  and  $m_2=15$  has been chosen (21 harmonics).

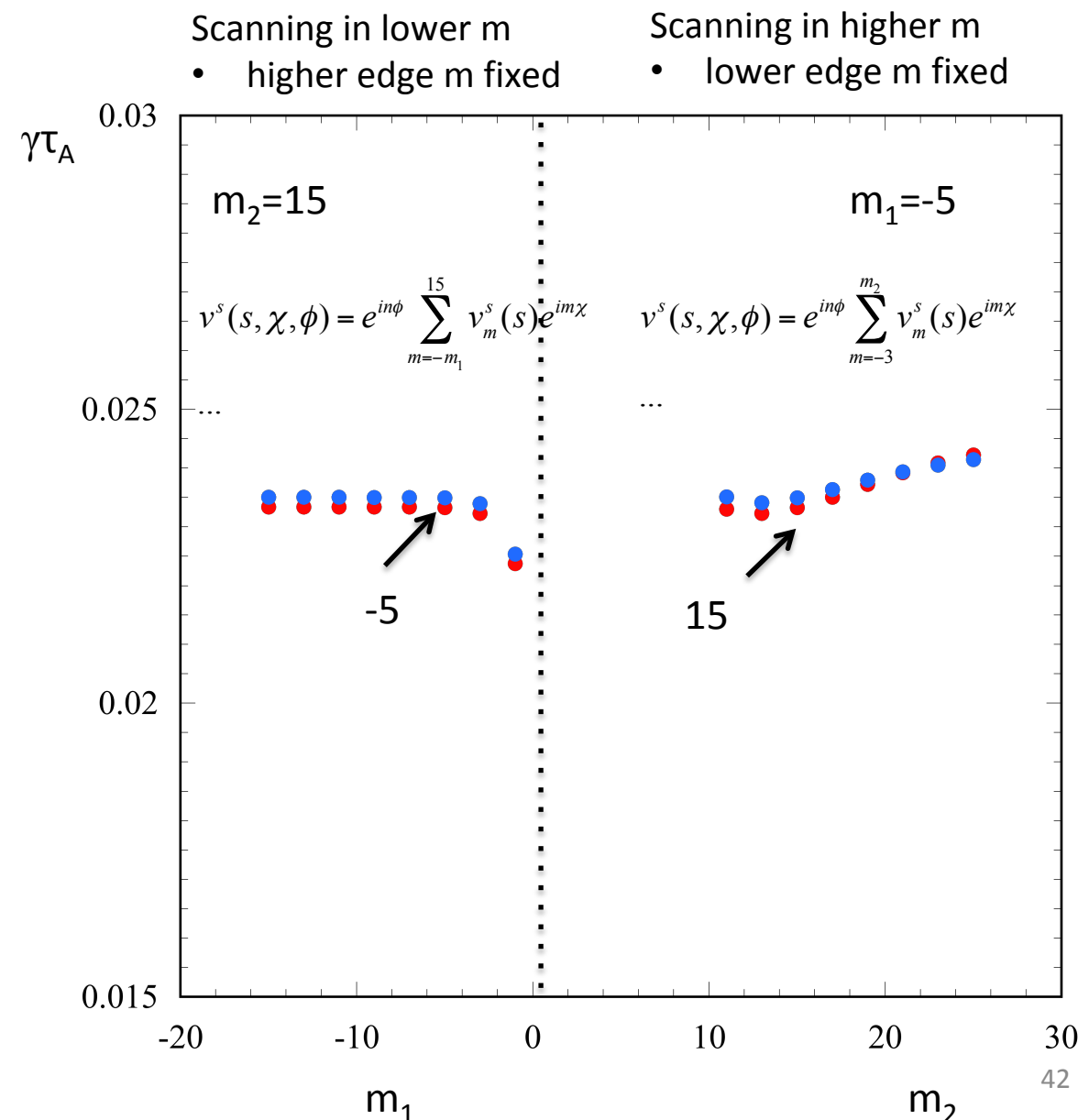


**Table 2**

PF Comparison among DTT, ITER and DEMO [30] main parameters.

	DTT	ITER	DEMO
R (m)	2.19	6.2	9.1
a (m)	0.70	2	2.93
A	3.1	3.1	3.1
I <sub>p</sub> (MA)	5.5	15	19.6
B (T)	6	5.3	5.7
Heating P <sub>tot</sub> (MW)	45	120	460
P <sub>sep</sub> /R (MW/m)	15	14	17
λ <sub>q</sub> (mm)	0.7	0.9	1.0
Pulse length (s)	100	400	7600

**Table 1**

Reference DTT physical parameters.

$n_e(10^{20} m^{-3})$	1.8
$n_e/n_G$	0.42
$P_{TOT}(MW)$	45
$\tau_E(z) H_{98} = 1$	0.43
$T_e(keV)$	6.1
$\beta(\%)$	2.2
$\nu^*(10^{-2})$	2.6
$\rho^*(10^{-3})$	2.9